

Extension of carbon flux estimation to oxic sediments based on sulphur geochemistry and analysis of benthic foraminiferal assemblages: A case history from the Eocene of Hungary

István Vető^{a,*}, Péter Ozsvárt^b, István Futó^c, Magdolna Hetényi^d

^a Geological Institute of Hungary, 1143 Budapest, Stefánia út 14, Hungary

^b Research Group for Paleontology, Hungarian Academy of Sciences—Hungarian Natural History Museum, Budapest, Hungary; P.O. Box 137, H-1431 Budapest, Hungary

^c Institute of Nuclear Research, 4026 Debrecen, Bem tér 18/c, Hungary

^d University of Szeged, P.O.Box 651, H-6701 Szeged, Hungary

Received 9 February 2006; received in revised form 21 September 2006; accepted 4 December 2006

Abstract

The amount and type of organic matter (OM), chemical and mineralogical compositions, and the amount and isotopic ratio of sulphur were measured and benthic foraminiferal assemblages were analysed in a 70 m thick core section comprising marine marls from the Eocene of Hungary. On the basis of Benthic Foraminiferal Oxygen Index (BFOI), the studied sediments were deposited under a range of anoxic to oxic bottom water conditions. The amount of C_{org} mineralised during early burial was calculated in two steps. First, carbon mineralised by sulphate reduction was calculated from the amount of sedimentary sulphur, corrected for escaped/oxidised H_2S by taking into account the isotopic composition of sulphur. Then, on analogy of recent sediments which are deposited with a similar rate of sedimentation and beneath bottom waters of similar O_2 content, carbon loss by aerobic respiration was estimated. A good stratigraphic control and knowledge of variation of mineralogical composition along the section permitted to estimate past variation of local organic carbon flux (C_{flux}) from calculated original C_{org} contents. During deposition of the studied strata, C_{flux} first decreased from 1.16 to 0.41 g $C_{org}/m^2/y$, then it progressively increased to 1.81 g $C_{org}/m^2/y$. Changes in local C_{flux} are explained by changes in water depth, flux of terrestrial organic components and availability of nutrients liberated by alteration of products of the coeval pyroclastic activity.

© 2006 Elsevier B.V. All rights reserved.

Keywords: Carbon flux; Sulphur isotope; Benthic foraminifers; Palaeoceanography; Eocene; Hungary

1. Introduction

Scientists dealing with ancient non-bioturbated sediments attempted to estimate past local organic carbon flux (C_{flux}) by calculating the bacterial loss of C_{org} from their sulphur content and taking into account the rate of sedimentation (SR) and density (ρ) (Littke et al., 1991; Vető and Hetényi, 1991; Lallier-Verges

* Corresponding author.

E-mail addresses: veto@mafi.hu (I. Vető), ozsi@nhmus.hu (P. Ozsvárt), futo@namafia.atomki.hu (I. Futó), hetenyi@geo.u-szeged.hu (M. Hetényi).

et al., 1993). Extending this approach to sediments deposited under more oxygenated conditions seems to be problematic due to increased difficulties in correction of C_{org} content for loss occurring during early burial.

In this work an estimation of C_{flux} prevailing during deposition of a Middle Eocene marginal marine section from the Hungarian Palaeogene Basin is attempted. While a minor part of the studied sediments was deposited beneath suboxic to anoxic bottom water, their bulk was formed under more oxygenated conditions. Therefore the sulphur-based approach introduced for non-bioturbated sediments (Littke et al., 1991; Vető and Hetényi, 1991; Lallier-Verges et al., 1993) needs to be modified, by taking into account the isotopic composition of sulphur and the oxidation of OM by aerobic respiration, too. Samples were collected at about every 1.5 m from a 70 m thick section of the Csetény 61 (Cs 61) borehole drilled in western Hungary (Fig. 1) in 1988.

First the geological setting will be briefly characterized, the applied chemical, isotopical, mineralogical and micropalaeontological methods will be described, and

principles and limitations of the calculation of C_{org} loss will be discussed in detail. In the next steps results will be reported and the observed trends will be compared with those of BFOI (Kaiho, 1994) and C_{flux} prevailing during deposition of the section will be discussed. Finally, factors governing the evolution of C_{flux} will be analysed.

2. Geological setting

The Hungarian Palaeogene Basin (HPB) is the largest Palaeogene basin remnant in the Eastern Alpine–Western Carpathian junction, shaped mostly by erosion and tectonic movements. Its preserved length is approximately 300 km (Fig. 1) (Kázmér et al., 2003). The basin contains Middle Eocene to Lower Miocene sediments, lavas and pyroclastics. Radiometric and fission-track dating suggest that the volcanic activity occurred between 44 to 30 Ma (Dunkl, 1990). This study focuses on the Middle Eocene strata of the NE Bakony, a part of the basin displayed on the inset map of Fig. 1. The geology of the NE Bakony is known in detail

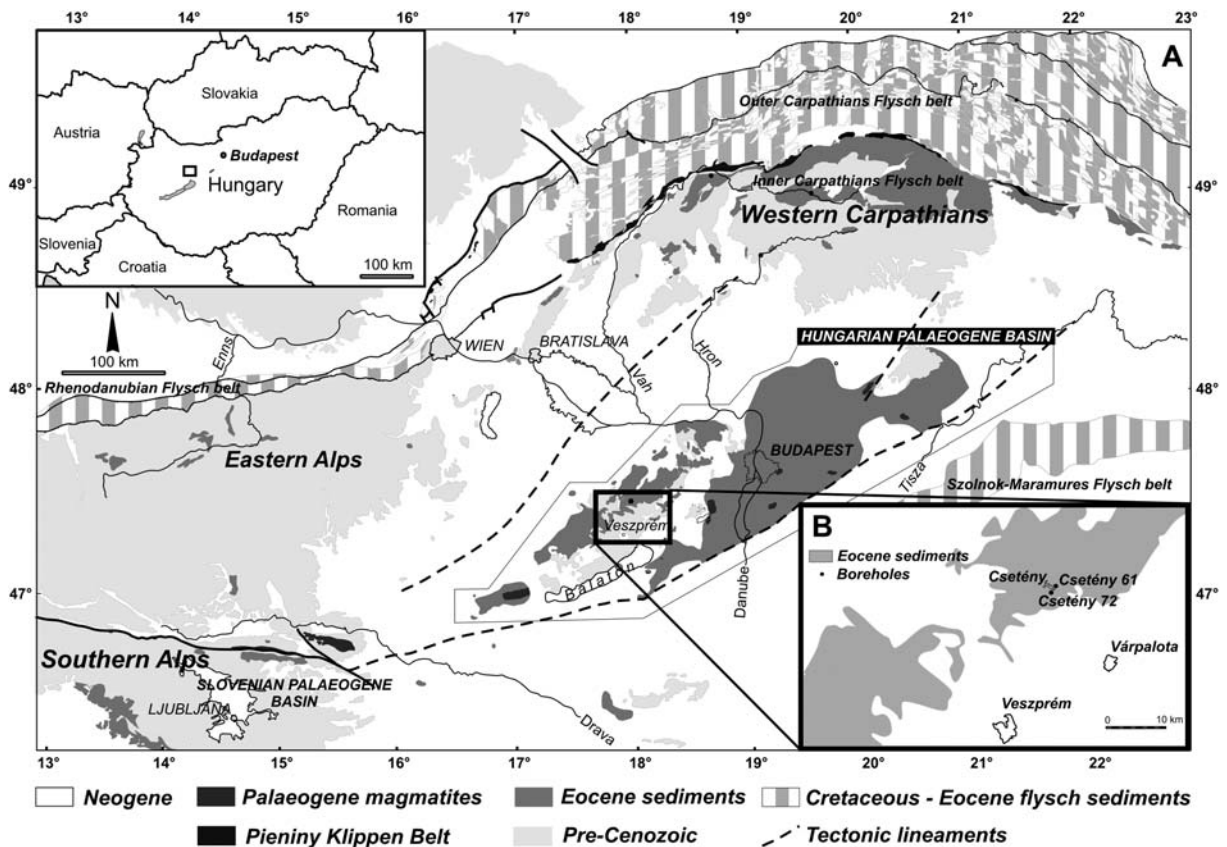


Fig. 1. A. Position of the Hungarian Palaeogene Basin in the Eastern Alpine–Western Carpathian junction (simplified after Kázmér et al., 2003). B. Location map showing the position of Csetény 61 and Csetény 72 boreholes.

from numerous boreholes drilled for exploring brown coal measures developed at the base of the Eocene.

Fig. 2 summarises the stratigraphy, with data from Báldi-Beke (nannoplankton; 1984), Horváth-Kollányi (planktic foraminifers; 1983) and Bernhardt et al. (lithostratigraphy; 1988).

During the late Lutetian–late Priabonian interval, the water depth continuously increased from shallow neritic to middle–lower bathyal (Báldi-Beke and Báldi, 1991). Using benthic foraminifera, Ozsvárt (2003) reconstructed the bottom water temperature and oxygenation trends for the same time period. Composition of the benthic foraminifera fauna and the results of the Q-mode principal factor analysis indicate warm, tropical conditions at the beginning of the Middle Eocene and a cooling during the late Middle Eocene and early Late Eocene. Estimated temperatures indicate temperate–cold conditions during this later period. On the basis of the Benthic Foraminiferal Oxygen Index (BFOI), the Middle and Late Eocene are characterized by two short and one longer eutrophic periods, separated by intervals of lower productivity. Sediments corresponding to eutrophic periods contain low-diversity faunas, with high dominance of infaunal low-oxygen tolerant species.

2.1. The Eocene of the Cs 61 borehole

The Cs 61 borehole penetrated 543 m, in which a 245 m thick Eocene succession was recovered. The oldest Eocene sediments (Fig. 3) at depth of 515.4 m are Upper Lutetian (NP16) gray clay, variegated clay and

clay marl layers frequently intercalated with thin coal seams (Dorog Formation). Above 476.0 m, this basal terrestrial sequence interfingers with calcareous marls and lumachelle of the Csernye Formation. At 470.0 m calcareous marls grade into grey, greenish grey marls of the Padrag Formation which is characterized by mass occurrence of coccoliths. Between 425.6 m and 420.6 m thin-bedded, laminated, fine-grained marls have been observed. Higher up (between 420.0 m and 401.0 m), stratification becomes more pronounced and the carbonate content increases. The upper part of the section is lithologically uniform, but the carbonate content of the marl layers is variable. The interval between 402.5 m and 356.0 m consists of thick-bedded marl, frequently intercalated with tuffaceous layers. At 269 m depth the Eocene is unconformably overlain by Upper Oligocene strata (Fig. 3).

3. Methods

3.1. Chemical and mineralogical measurements

About 20–30 g from each core sample was ground in a Fritsch ball mill. Total organic carbon content (TOC), Hydrogen Index (HI) and T_{max} were determined on a Delsi Oil Show Analyser under standard conditions at the Dept. of Mineralogy, Geochemistry and Petrography of the University of Szeged.

Chemical and mineralogical analyses were carried out at the laboratories of the Geological Institute of Hungary. Total sulphur (TS) and Ba contents were measured by ICP-AES technique after fusion with Li-metaborate.

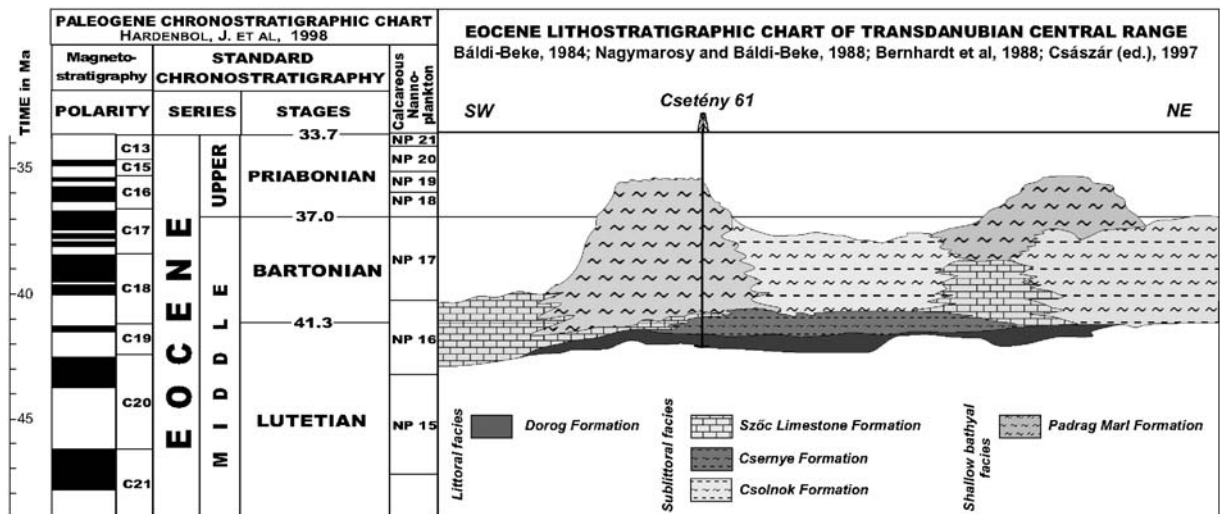


Fig. 2. Eocene lithostratigraphy (after Báldi-Beke, 1984; Nagymarosy and Báldi-Beke, 1988; Bernhardt et al., 1988 and Császár (Ed.), 1997) and chronostratigraphy (after Hardenbol et al., 1998) in the area of the Eastern Bakony.

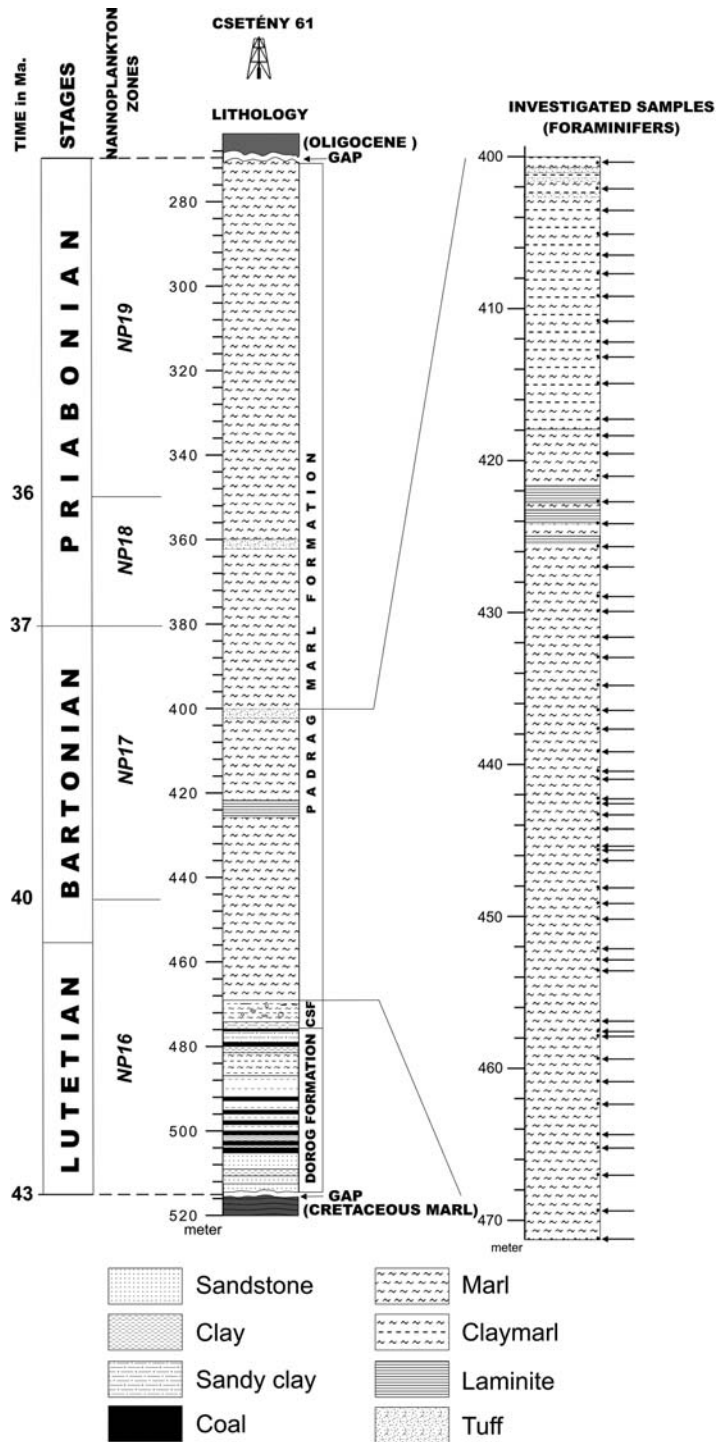


Fig. 3. Stratigraphy and lithology of the Eocene sequence in Csetény 61 borehole. Biostratigraphical and lithostratigraphical data from Kollányi et al., 2003.

Uncertainties of the measurements were ± 10 and $\pm 20\%$, respectively. The X-ray diffraction analyses were done on a Philips PW 1730 diffractometer under the following

conditions: Cu anti-cathode, 40 kV and 30 mA tube-current, graphite monochromator, goniometer speed $2^\circ/\text{min}$. The mineral composition was calculated on the

basis of the relative intensity rates of the reflections characteristic of the minerals, applying the published or experimental corundum factors on minerals.

Total sulphur for isotope ratio measurement was extracted by fusion with a soda- NaNO_3 mixture and the sulphate obtained was precipitated as BaSO_4 . After weighing the BaSO_4 preparatum was analysed (off line preparation) following the method introduced by Halas et al. (1982) for the determination of sulphur isotope ratio, which was measured against the NSB-121 and NBS-127 barite standards on a high precision McKinney–Nier type stable isotope ratio mass spectrometer developed in the Institute of the Nuclear Research of the Hungarian Academy of Sciences in Debrecen. The equipment is provided with two ion sources (H, CNOS sources) and ten separate Faraday cups. Trap regulation of a magnetically and electrostatically focused electron beam is used to achieve stable ion production in the ion source. Mass setting is performed by varying the ion accelerating voltage. A symmetrical dual viscous inlet system has been constructed for measuring the sample and standard gases alternatingly. Pneumatically actuated bakeable gold sealed metal valves exclude cross mixing between sample and standard gases. For further technical details the readers are referred to Hertelendi et al. (1986). The S isotope measurements are given in the δ -notation relative to the VCDT standard. Replicate analyses agreed within $\pm 0.2\%$.

3.2. Foraminiferal analysis

Approximately 250–300 g from each core sample was cleaned using hydrogen peroxide. The residues were washed over a 50 μm sieve and dried. Samples were divided into the grain-size fractions of 50–500 μm and $>500 \mu\text{m}$. Faunal analysis was performed only on the 50–500 μm fraction. Prior to separation and counting, the samples were divided into parts of 1/2; 1/4; 1/8 etc., using a micro-splitter. For faunal analysis, ~ 200 –250 specimens were picked, unless their numbers were less than 200, in which case all specimens were picked.

For palaeoecological and palaeoceanographical studies, the Benthic Foraminiferal Number (BFN), Diversity ($H(S)$), Plankton/Benthos ratio ($P/P+B$) were calculated, Benthic Foraminiferal Oxygen Index (BFOI) and Q-mode (Varimax-rotated) principal factor analysis was applied.

The BFN parameter is the number of specimens per gram sediments (Schott, 1935) and gives an indication of the sedimentation rate, productivity and carbonate dissolution (Douglas and Woodruff, 1981). In dysoxic environments and on the continental margin the BFN is

not reflecting organic carbon fluxes to the sea floor accurately (Naidu and Malmgren, 1995; Den Dulk et al., 2000; Mühlstrasser, 2001), therefore we used BFOI for the estimation of changes in bottom water oxygenation. The values of the index were calculated using Kaiho's (1994) equations. The detailed description of calculation is given in Kaiho (1994, 1999). The BFOI reflects the estimated dissolved oxygen levels in recent ocean water which is based on proportion of the different microhabitat preference of the benthic foraminifera. The estimated dissolved oxygen levels for the Palaeogene bottom water is based on the comparison with morphologically similar extant foraminifera taxa according to Corliss (1985, 1991), Corliss and Chen (1988), Kaiho et al. (2006). However, Kaiho (1991) already used dissimilarity of benthic foraminiferal test morphology to extrapolate relative amounts of dissolved oxygen in the world oceans from early Eocene to late Oligocene times. Scherbacher et al. (2001) and Schmiedl et al. (2002) also estimated the dissolved oxygen levels in bottom water of the Paratethys from the Inneralpine Molasse Basin and from the Slovenian Palaeogene Basin (Fig. 1). Kaiho et al. (2006) divided some Palaeocene–early Eocene calcareous benthic foraminifera into dysoxic (0.1–0.3 O_2 ml/l) suboxic (0.3–1.2 O_2 ml/l) and oxic ($>1.2 \text{O}_2$ ml/l) indicators on the basis of relations between specific morphologic characters and calcareous benthic foraminiferal microhabitat and oxygen levels. If the BFOI value is bigger than 50, it corresponds to highly oxic environment (dissolved oxygen >3.0 ml/l). If the BFOI values are between 0 and 50, based on dysoxic, suboxic and a low ratio of oxic species, it corresponds to less oxic environments (dissolved oxygen is between 1.5 and 3.0 ml/l). If the BFOI values are between -40 and 0, based on dysoxic and a high ratio of suboxic species, it corresponds to suboxic environment (dissolved oxygen is between 0.3 and 1.5 ml/l, see Fig. 4). If the BFOI values are between -50 and -40 , based on dysoxic and low ratio of suboxic species, it corresponds to dysoxic environments (dissolved oxygen is between 0.1 and 0.3 ml/l, see Fig. 4). If the calcareous benthic foraminifera are absent, the BFOI is -55 (Kaiho, 1994, 1999).

Diversity, i.e. the stability of an ecosystem, was measured using the Shannon–Wiener $H(S)$ index (Buzas and Gibson, 1969).

The ratio between planktic and sum of planktic and benthic foraminifera ($P/P+B$) is one of the most reliable proxies to estimate palaeo-water depth during deposition. Grimsdale and Van Morkhoven (1955), Boltovskoy and Wright (1976), Gibson (1989) and Van der Zwaan et al. (1999) demonstrated that the percentage of planktic foraminifera in surface sediments increases

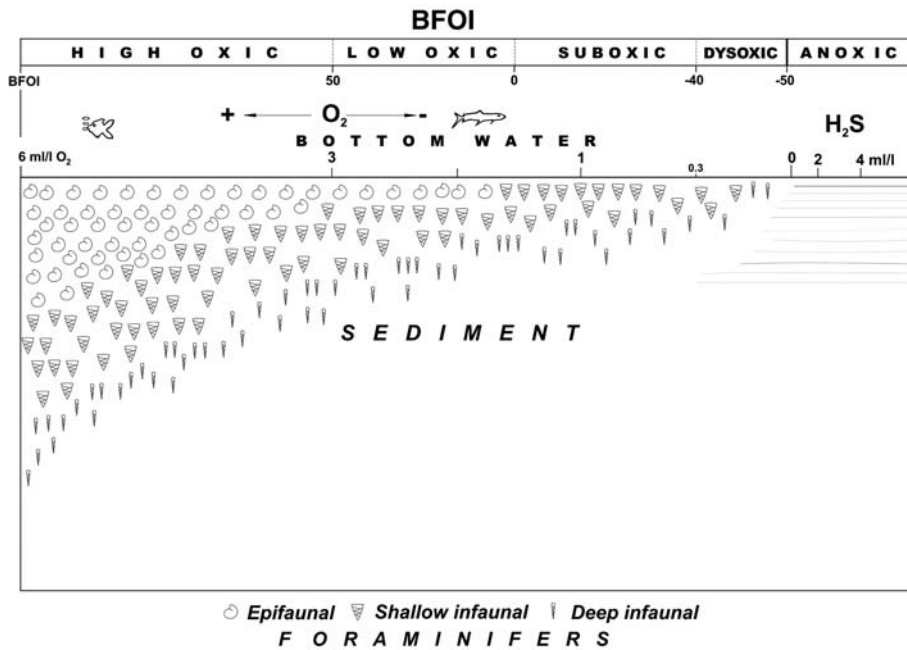


Fig. 4. The BFOI model. For discussion, see text (after Kaiho, 1994, 1999).

with water depth. One limitation of the method is obvious: the depth range that can be reconstructed is between 0 and 1200 m, because at greater depth the assemblage is almost completely dominated by planktic foraminifers (Van der Zwaan et al., 1999).

We distinguished foraminiferal associations by Q-mode principal factor analysis with subsequent Varimax rotation. With this method, the complex number of variables (species) is reduced to a small number of independent variables (factors). The factor loadings matrix and factor scores matrix are necessary for the interpretation of the data set. Factor loadings >0.4 (Malmgren and Haq, 1982) are supposed to indicate statistically significant dependence of the distribution of benthic foraminiferal assemblages (factors) on the combination of specific environmental variables (Wollenburg and Mackensen, 1998). The factor scores show the importance of a species within a factor. The values of scores greater than 4 are assigned to dominant taxa, and factor scores between 1 and 4 to important associated taxa of an assemblage. The statistics software package SYSTAT 10.2 was used for statistical calculations.

4. Principles and limitations of calculation of original C_{org} content

Knowledge of original C_{org} content (TOC_{or}), rate of sedimentation (SR), and sediment density (ρ) offers a tool for quantitative estimation of C_{flux} and its changes.

While ρ of ancient sediments is satisfactorily known in most cases, their TOC_{or} and/or SR are often only known with a high degree of uncertainty. Here only the problem of TOC_{or} is addressed.

The relationship between TOC and TOC_{or} is expressed by the following equation:

$$\text{TOC}_{\text{or}} = \text{TOC} + \Delta\text{TOC}_{\text{th}} + \Delta\text{TOC}_{\text{bact}} \quad (1)$$

where $\Delta\text{TOC}_{\text{th}}$ and $\Delta\text{TOC}_{\text{bact}}$ are amounts of organic carbon lost by thermal and bacterial degradation, respectively. In case of immature sediments, the amount of $\Delta\text{TOC}_{\text{th}}$ is insignificant. On the other hand, $\Delta\text{TOC}_{\text{bact}}$ is important in most cases and can be even greater than TOC. $\Delta\text{TOC}_{\text{aer}}$ and $\Delta\text{TOC}_{\text{anaer}}$ are amounts of organic carbon lost by aerobic and anaerobic bacterial processes, respectively and their sum equals $\Delta\text{TOC}_{\text{bact}}$.

Usually, bacterial degradation of OM starts in oxic environment then, after exhaustion of the oxygen dissolved in pore water, continues in an anoxic one. Bacterial degradation of OM via aerobic oxidation is described by the following equation:

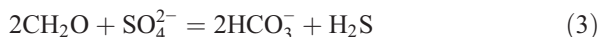


This reaction results in a decrease of the pore water pH and is accompanied by carbonate dissolution (e.g. Raiswell, 1997).

Bacterial degradation of OM via reduction of sulphate of seawater origin is by far the most important

among the anaerobic bacterial reactions, therefore the amount of organic carbon lost due to sulphate reduction ($\Delta\text{TOC}_{\text{sulf}}$) can be considered as equalling $\Delta\text{TOC}_{\text{anaer}}$.

Sulphate reduction is described by the following equation:



This reaction is accompanied by a substantial sulphur isotope fractionation (Vinogradov et al., 1962; Kaplan et al., 1963) and results in an increase of the pore water pH and formation of iron sulphides (mainly pyrite) and carbonates (Raiswell, 1997). Therefore, in contrast to the aerobic oxidation, sulphate reduction produces a mineralogical record preserved in the sediments.

4.1. Estimation of TOC_{or} in immature, non-bioturbated sediments

If aerobic oxidation is not significant, as is the case in non-bioturbated sediments, sulphate reducers are responsible for the bulk of the degradation thus the amount of H_2S produced is proportional to $\Delta\text{TOC}_{\text{bact}}$ (Littke et al., 1991; Vető and Hetényi, 1991; Lallier-Verges et al., 1993). A part of this H_2S , isotopically lighter than the parent sulphate, is fixed in the sediments as reduced sedimentary sulphur (S_{red}), mostly in pyrite and OM without any significant isotope fractionation, the sulphate is enriched in ^{34}S , whereas the remaining H_2S escapes the site of sulphate reduction and is oxidised to sulphate (Rozanov et al., 1971; Goldhaber and Kaplan, 1980), elemental sulphur, thiosulphate and sulphite (Jørgensen, 1990; Canfield and Thamdrup, 1994; Habicht et al., 1998). According to the atomic weights of carbon and sulphur and to the stoichiometry of sulphate reduction described by the Eq. (3) one can calculate $\Delta\text{TOC}_{\text{sulf}}$ and TOC_{or} using the following equations:

$$\Delta\text{TOC}_{\text{sulf}} = \text{S}_{\text{red}} \times 75 / (100 - \Delta\text{H}_2\text{S}) \quad (4)$$

and replacing $\Delta\text{TOC}_{\text{bact}}$ with $\text{S}_{\text{red}} \times 75 / (100 - \Delta\text{H}_2\text{S})$ TOC_{or} can be estimated using the below equation:

$$\text{TOC}_{\text{or}} = \text{TOC} + \text{S}_{\text{red}} \times 75 / (100 - \Delta\text{H}_2\text{S}) \quad (5)$$

where $\Delta\text{H}_2\text{S}$ is the amount of lost/oxidised H_2S expressed in percentage of the total produced.

In non-bioturbated sediments and in sediments where bioturbation has already ceased, the escape of H_2S and the replenishment of the porewater by sulphate are assured by upward and downward diffusion, respec-

tively. Here we note that a part of S_{red} can be produced by processes that are not based on dissolved sulphate of direct seawater origin and which will be discussed briefly in Section 4.3. On the basis of distribution of sulphate and sulphide in porewater along depth in 12 relatively organic-rich recent marine sediment profiles, in absence of bioturbation, the amount of diffusively lost H_2S is seldom more than 25% of the total produced (Vető et al., 1995). Vető et al. (2000) have estimated TOC_{or} for the non-bioturbated Upper Triassic Kössen Marl (W. Hungary) by replacing $\Delta\text{H}_2\text{S}$ with 25% in Eq. (5).

4.2. Difficulties of TOC_{or} estimation in immature bioturbated sediments and a new solution

In bioturbated sediments, escape and oxidation of H_2S produced are more intense than in non-bioturbated ones and aerobic mineralisation of OM is significant or even dominant. First the problem of $\Delta\text{H}_2\text{S}$ estimation should be addressed.

If the porewater sulphate is entirely reduced to H_2S which in turn is entirely fixed as S_{red} , this later has obviously the same isotopic composition as the parent sulphate.

S_{red} content of marine sediments in many cases is significantly higher than the amount of sulphur introduced by the porewater sulphate at the time of deposition and its $\delta^{34}\text{S}$ is significantly lower than that of the parent sulphate. These observations together mean that a non-negligible amount of sulphate enters the sediments after their deposition and a part of the corresponding sulphur, enriched in ^{34}S relative to the parent sulphate escapes the sediments (Zaback et al., 1993). Hence, one can assume that the magnitude of $\Delta\text{H}_2\text{S}$ is by some way related to the net S-isotope fractionation between S_{red} and parent sulphate ($\Delta^{34}\text{S}_{\text{sulphate-sulphide}}$). Isotope mass balance considerations of Zaback et al. (1993) suggest that the higher is the percentage of H_2S escaping the sediment ($\Delta\text{H}_2\text{S}$), the greater is $\Delta^{34}\text{S}_{\text{sulphate-sulphide}}$.

Direct oxidation of the escaping H_2S furnishes isotopically light sulphate for further bacterial reduction. Studies carried out by Jørgensen (1990), Canfield and Thamdrup (1994) and Habicht et al. (1998) revealed that elemental sulphur, thiosulphate and sulphite can be important reaction intermediates of sulphide oxidation. The relative weights of direct sulphide oxidation and the above listed intermediate reactions can significantly vary between different depositional settings (Habicht and Canfield, 2001). Bacterial disproportionation of these compounds to sulphate and sulphide is accompanied by significant isotope fractionation resulting in ^{34}S -depleted H_2S . Hence, both the isotopically light sulphate, produced

by direct oxidation of H_2S , and the isotopically very light H_2S generated by disproportionation of the above reaction intermediates contribute to formation of ^{34}S -depleted sedimentary sulphides.

Canfield and Teske (1996) have calculated sulphide loss for 17 recent non-photosynthetic marine sediment samples as the percentage difference between the depth-integrated rate of sulphate reduction measured directly with radiotracer and the rate of sulphur burial (as pyrite and acid-volatile sulphide phases). It is worth to note that the term “percentage sulphide oxidation” is used by them as an equivalent of “percentage sulphide loss” (see legend and X axis of their Fig. 2a). They have found that in the studied sediments percentage of sulphide loss is a linear function of $\Delta^{34}\text{S}_{\text{sulphate-sulphide}}$ ($R^2=0.888$) but have not given the equation describing the relationship of the two parameters. Since the corresponding data pairs are not tabulated, we have read them off and calculated the equation as follows:

$$\Delta\text{H}_2\text{S} = 2.928 \times \Delta^{34}\text{S}_{\text{sulphate-sulphide}} - 58.21 \quad (R^2 = 0.888) \quad (6)$$

Data of Canfield and Teske (1996) and the best fit line corresponding to Eq. (6) are displayed on Fig. 5.

Eq. (6) is an empirical expression of the relationship between $\Delta\text{H}_2\text{S}$ and $\Delta^{34}\text{S}_{\text{sulphate-sulphide}}$, controlled by multiple processes operating in the reductive and mainly in the oxidative part of the sulphur cycle. Its use for calculating $\Delta\text{H}_2\text{S}$ is limited for several reasons.

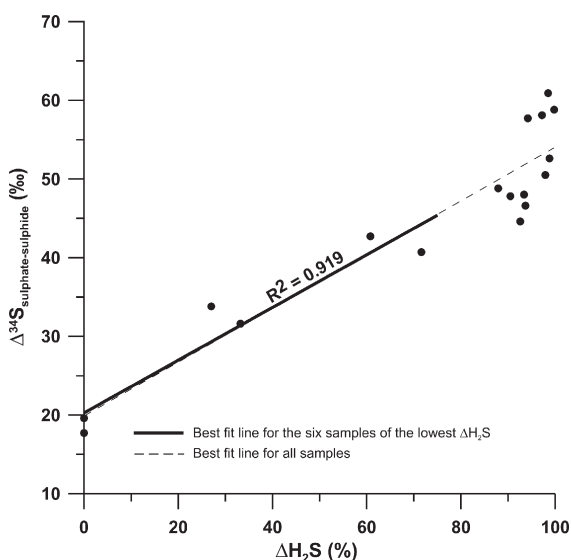


Fig. 5. Variation of $\Delta^{34}\text{S}_{\text{sulphate-sulphide}}$ in function of $\Delta\text{H}_2\text{S}$ in recent marine sediments (After Fig. 2a of Canfield and Teske, 1996).

Eq. (6) is not suitable for estimation of TOC_{or} in photosynthetic sediments since their area displayed on Fig. 2a of Canfield and Teske (1996) is significantly below the band of the 17 sediment samples. These authors point out that the oxidative part of the sulphur cycle of photosynthetic sediments is very different from that of the non-photosynthetic ones, but the discussion of this question is beyond the scope of this paper.

Canfield and Teske (1996) have not considered organically bound sulphur in the calculation of the rate of sulphur burial, hence the use of Eq. (6) for estimating $\Delta\text{H}_2\text{S}$ in sediments characterized by sulphur-rich OM is very problematic.

Eq. (6) is expressing the relationship between $\Delta\text{H}_2\text{S}$ and $\Delta^{34}\text{S}_{\text{sulphate-sulphide}}$ for a $\Delta^{34}\text{S}_{\text{sulphate-sulphide}}$ interval between 20 and 54‰ and does not give meaningful estimation of $\Delta\text{H}_2\text{S}$ neither in case of $\Delta^{34}\text{S}_{\text{sulphate-sulphide}} > 54‰$ ($\Delta\text{H}_2\text{S}$ would be above 100%) nor in case of $\Delta^{34}\text{S}_{\text{sulphate-sulphide}} < 20‰$ ($\Delta\text{H}_2\text{S}$ would be negative). On the other hand, in the case of relatively high $\Delta^{34}\text{S}_{\text{sulphate-sulphide}}$ values (around 50‰) small changes in $\Delta^{34}\text{S}_{\text{sulphate-sulphide}}$ led to important changes in $\Delta\text{TOC}_{\text{sulf}}$ estimation. For example, an increase of $\Delta^{34}\text{S}_{\text{sulphate-sulphide}}$ from 50 to 52‰ results in an increase of $\Delta\text{H}_2\text{S}$ from 88 to 94%. Replacement of $\Delta\text{H}_2\text{S}$ with these values in Eq. (4) results in a twofold increase of $\Delta\text{TOC}_{\text{sulf}}$. It is easy to understand that using Eq. (6) for samples showing $\Delta^{34}\text{S}_{\text{sulphate-sulphide}}$ around 50‰ would lead to unreasonably high $\Delta\text{TOC}_{\text{sulf}}$ values.

In view of these problems we have somehow arbitrarily chosen the six samples of Fig. 5, characterized by the lowest $\Delta^{34}\text{S}_{\text{sulphate-sulphide}}$ values and recalculated Eq. (6) for them. The obtained new equation

$$\Delta\text{H}_2\text{S} = 2.985 \times \Delta^{34}\text{S}_{\text{sulphate-sulphide}} - 60.48 \quad (R^2 = 0.919) \quad (7)$$

is surprisingly similar to Eq. (6). This close similarity means that formal validity interval of Eq. (7) practically equals that of Eq. (6) and the problem of very fast increase of $\Delta\text{H}_2\text{S}$ with increasing $\Delta^{34}\text{S}_{\text{sulphate-sulphide}}$ at the higher end of the validity interval is still persisting. It is very probable that the precise numerical value of $\Delta^{34}\text{S}_{\text{sulphate-sulphide}}$ corresponding to 100% $\Delta\text{H}_2\text{S}$ is not of great importance and estimation of $\Delta\text{TOC}_{\text{sulf}}$ for fossil sediments showing high $\Delta^{34}\text{S}_{\text{sulphate-sulphide}}$ can be carried out only with some simplification.

Here the following simplifying solution will be used for estimation of $\Delta\text{H}_2\text{S}$ in case of high $\Delta^{34}\text{S}_{\text{sulphate-sulphide}}$: if $\Delta^{34}\text{S}_{\text{sulphate-sulphide}}$ is higher than a defined value, $\Delta^{34}\text{S}_{\text{sulphate-sulphide}}$ has to be replaced with this value in Eq. (7). Since Eq. (7) has been obtained for the six

samples of Fig. 5 having the lowest $\Delta^{34}\text{S}_{\text{sulphate-sulphide}}$ values, 45‰, the lowest $\Delta^{34}\text{S}_{\text{sulphate-sulphide}}$ shown by the remaining 11 samples will be used as the defined value. It is obvious that $\Delta\text{TOC}_{\text{sulf}}$ obtained by this way will be underestimated. It is easy to understand that this underestimation is an improvement of the approach using Eq. (4) as it has been proposed by Lallier-Verges et al. (1993) and Littke et al. (1991); their approach implies that S_{red} is considered as representing the whole amount of H_2S produced by sulphate reducers.

Eq. (8) cannot be used for photosynthetic sediments and for sediments containing sulphur-rich OM. If isotope compositions of S_{red} and the parent seawater sulphate are known, $\Delta\text{TOC}_{\text{sulf}}$ can be calculated using the following modified version of Eq. (4):

$$\Delta\text{TOC}_{\text{sulf}} = S_{\text{red}} \times 75 / (160.48 - 2.985 \times \Delta^{34}\text{S}_{\text{sulphate-sulphide}}) \quad (8)$$

where $\Delta^{34}\text{S}_{\text{sulphate-sulphide}}$ has to be replaced with 45‰ if sulphur isotope fractionation is over 45‰.

Since aerobic mineralisation of OM does not result in precipitation of autigenic minerals, a direct estimation of $\Delta\text{TOC}_{\text{aer}}$, as proposed for that of $\Delta\text{TOC}_{\text{sulf}}$, is not possible. The causal relationship between conditions of sedimentation and the $\Delta\text{TOC}_{\text{aer}}/\Delta\text{TOC}_{\text{anaer}}$ ratio offers an indirect way for this estimation. According to Canfield (1994), SR and the bottom water O_2 content exert strong control on relative weights of aerobic and anaerobic mineralisation of OM. He points out that relative weight of aerobic mineralisation increases with both the increase of bottom water O_2 content and decrease of sedimentation rate. This relationship is reflected by the difference in OM mineralisation between normal deep-sea sediments, deposited slowly under well-oxygenated bottom water, and sediments deposited on continental margins, characterized by rapid burial and low-oxygen bottom water. In deep-sea setting, in most cases the aerobic respiration represents the greater or even the major part of carbon oxidation, whereas the anaerobic process plays generally the leading role in carbon oxidation in continental margin sediments. The double control exerted on $\Delta\text{TOC}_{\text{aer}}/\Delta\text{TOC}_{\text{anaer}}$ ratio by SR and bottom water O_2 content is not expressed yet in a numerical formula, therefore in ancient sediments $\Delta\text{TOC}_{\text{aer}}$ can be assessed only empirically, by multiplying $\Delta\text{TOC}_{\text{sulf}}$ calculated by Eq. (7) which practically equals $\Delta\text{TOC}_{\text{anaer}}$ with the $\Delta\text{TOC}_{\text{aer}}/\Delta\text{TOC}_{\text{anaer}}$ ratio determined in recent sediments deposited beneath waters of similar O_2 content and with SR similar to those prevailing during deposition of the studied ancient sediments.

4.3. Additional reduced sulphur species

4.3.1. Syngenetic pyrite

In sulphidic seawater bacterial sulphate reduction is operating. The sulphide generated is fixed in pyrite in the water column which accumulates on the sea-floor together with terrigenous and planktonic sedimentary matter. The amount of the corresponding sulphur can be as high as 1.5% in the recent sediments of the Black Sea (Leventhal, 1983).

Due to the unlimited sulphate reservoir of the oceans the $\Delta^{34}\text{S}_{\text{sulphate-sulphide}}$ of the pyrite precipitated in the seawater practically equals the fractionation accompanying the sulphate reduction, that is reflected by the very negative $\delta^{34}\text{S}$ of the S_{red} in euxinic sediments like in some Mediterranean sapropels studied by Passier et al. (1999).

Since the sulphate reduction responsible for syngenetic pyrite takes place in the water column, the accompanying oxidation of C_{org} does not result in a diminution of TOC. Hence the amount of the corresponding S_{red} should not be considered in estimation of $\Delta\text{TOC}_{\text{sulf}}$.

4.3.2. S_{red} produced by reduction of baritic sulphate

Micro-crystalline barite is present in relatively high amount (up to 7–9%) in the carbonate-free fraction of sediments of some high productivity areas of the oceans (Torres et al., 1996). This barite is probably precipitated within microenvironments of biological debris settling down through water column and has the same $\delta^{34}\text{S}$ as the seawater sulphate (Paytan et al., 1998). This biogenic barite is widely used as a geochemical proxy for palaeoproductivity (Dymond et al., 1992).

Due to exhaustion of dissolved sulphate at the base of the sulphate reduction zone pore water becomes undersaturated for barite and a portion of the biogenic barite is dissolved. The sulphate liberated is reduced to sulphide which behaves as does the sulphide produced by reduction of the “normal” pore water sulphate. Consequently the small portion of S_{red} corresponding to the dissolved barite can be taken into consideration without any special attention in estimating $\Delta\text{TOC}_{\text{sulf}}$.

4.3.3. S_{red} produced by reduction of sulphate, sourced by anoxic oxidation of pyrite

Bottrell et al. (2000) report isotopic evidences for anoxic pyrite oxidation by Fe^{3+} minerals in sediments of the Cascadia margin. These authors suggest that the resulting sulphate can feed bacterial activity below the zone of bacterial methane oxidation and the corresponding H_2S would be fixed as S_{red} . On the other hand, experimental work of Schippers and Jørgensen

(2002) casts doubt if Fe^{3+} minerals would be able to oxidize pyrite in anoxic environment. Consequently, this kind of S_{red} , obviously of secondary importance will not be considered further.

5. Results

5.1. Organic matter, sulphur and mineralogical composition

TOC, TS content, sulphur isotope ratio ($\delta^{34}\text{S}$), and Hydrogen Index (HI) are listed in Table 1 and mineralogical compositions are listed on Table 2. Sulphur contents weighed as BaSO_4 (TS_{grav}) are also listed in Table 1. Changes of carbonate, TOC and TS contents, $\delta^{34}\text{S}$, and HI in function of depth are displayed on Fig. 6. On the basis of carbonate, TS, TOC and HI patterns the section is divided into three parts.

The lower part (470.5–447 m) that belongs to the NP16 nannozone is characterized by upward decrease of TOC (from 1.1 to 0.2%) and TS content (from 1.19 to 0.32%) and the HI (from 180 to 40 mg HC/g TOC), and an upward increase of carbonate content (from 23 to 63%). At 447 m the carbonate content drops markedly.

In the middle part (447–435.5 m) none of the above four parameters shows a clear depth trend and the carbonate and TS contents show a relatively large scatter (20 to 50% and 0.22 to 0.69%, respectively), whereas TOC and HI are low (<0.5% and <80 mg HC/g TOC, respectively) and vary less significantly. It is worth to mention that the sample from 445.6 m shows exceptionally high TOC and HI.

The upper part (435.5 to 400.5 m) is separated from the middle one by a pronounced fall in carbonate content and a similarly marked jump in TOC. Carbonate is low relative to the rest of the section and shows only small variation up to 410 m where it starts to increase slightly. TOC and HI first increase from 0.6 to 1.4% and from 65 to 160 mg HC/g TOC, respectively, then show pronounced reversals at around 413 m and start to rise again but with a relatively great scatter. TS content increases upwards (from 0.47 to 1.17%) but with a high scatter.

$\delta^{34}\text{S}$ very slightly increases upward up to 435.5 m with a significant variation between -35 to -17% . Above 435.5 m its curve shows a rapid alternation of increasing and decreasing segments in which the $\delta^{34}\text{S}$ gradient can be as high as 15‰/m (Fig. 6).

The low T_{max} values (403 to 427 °C) suggest that the OM is immature throughout the interval. Sparse data (Cs. Sajgó written comm. 2006) show that organic C/N ratio decreases upward through the lower and middle parts of the section (Fig. 6).

BaO content ranges between 0.011 to 0.041%. Assuming that Ba is entirely fixed in barite, what is obviously not the case, the amount of baritic sulphur would be max. 0.008%. Biogenic carbonates contain minor amount of sulphate in lattice sites. 436 ppm, the average concentration of sulphatic sulphur in the bulk carbonate of 12 recent marine sediment samples (Burdett et al., 1989) can be used for estimating the sulphatic sulphur content of the bulk carbonate in the Cs 61 section. Since the samples taken from this section contain 15 to 63% biogenic carbonate, the corresponding amount of lattice bound sulphatic sulphur varies between 0.007 and 0.027%. Gypsum, present mostly in traces but in some samples in measurable amounts (Table 2), has been obviously produced by oxidation of pyrite, which took place during the 15 yr of storage of the core material in a core repository. Hence the measured TS contents practically represent the S_{red} contents of the fresh core material. A part of the S_{red} is obviously organically bound (S_{org}). Sulphur-rich OM is of Type I or Type II (Orr, 1986), rich in hydrogen. According to HI values, ranging between 38 and 180 mg HC/g TOC (Table 1), the studied samples contain Type III OM, poor in hydrogen. In view of the TOC range (0.14–1.51%, Table 1), and considering the high C/S ratio of Type III OM, (the average of the C/S ratios reported by Durand and Monin (1980) for three immature Type III kerogen samples is 28), the amount of S_{org} is of minor importance.

Common presence of aragonite proves that the syngenetic carbonate was not altered during diagenesis. The clay mineral assemblage consists of montmorillonite, illite/smectite, illite and chlorite and kaolinite. Strong variation of the carbonate content masks a compositional variation of the carbonate-free, mostly terrigenous portion along the section.

The amount of plagioclase is significantly higher above 440 m than below this depth (Table 2). The increased plagioclase content above 440 m reflects a significant contribution of pyroclastic material. Sparse presence of zeolite supports this assumption.

5.2. Foraminiferal analyses

The benthic foraminifera fauna of the studied section is characterized by shallow to deep infaunal genera (e. g. *Bulimina*, *Uvigerina*, *Lenticulina* and *Bolivina*). Epifaunal genera (e. g. *Cibicides*, *Cibicidoides* and *Heterolepa*) are characteristic between 434 m and 462 m.

5.2.1. $H(S)$

The Shannon–Wiener $H(S)$ diversity index of the benthic foraminiferal association varies between 1 and 3 (Fig. 7). In the lower part of the section (between 432 m

Table 1
TOC, TS, TS_{grav}, sulphur isotope ratio ($\delta^{34}\text{S}$), and Hydrogen Index (HI) data

Depth (m)	TS (%)	TS _{grav} (%)	$\delta^{34}\text{S}$ (‰)	TOC(%)	HI (mg HC/g TOC)
400.50	1.17	1.34	-21.7	1.40	144
402.00	1.08	1.23	-25.4	1.10	115
403.60				1.06	100
405.00	1.16	1.29	-13.3	1.51	158
406.50				1.21	119
407.80	1.21	1.40	-10.6	0.81	97
409.20	1.22	1.43	-4.1	0.94	88
410.70				0.89	85
412.10	0.86	1.01	-19.0	0.92	91
413.40				1.39	120
415.10	0.89	1.04	-27.2	1.24	141
416.60	1.03	1.25	-25.9	1.24	121
418.20	1.18	1.43	-34.5	1.25	132
419.70	1.04	1.18	-8.5	1.11	123
*420.90		1.11		0.85	97
421.20	1.10	1.34	9.6	0.91	92
*421.60		1.07		0.86	90
422.70	1.22	1.43	3.3	0.93	81
*422.80		0.71		0.80	68
*424.00		1.16		0.72	63
424.20	0.69	0.83	-6.3	0.95	84
425.70	1.10	1.30	-2.0	0.83	80
427.00	0.84	0.99	-19.2	0.78	71
428.90	0.66	0.77	-14.2	**0.88	82
430.00				0.86	73
431.70	0.47	0.57	-17.3	0.70	72
433.20				0.62	69
434.70	0.79	0.99	-28.2	**0.69	66
436.40	0.22	0.25	-16.8	0.18	52
437.90	0.55	0.69	-31.0	0.14	71
439.20	0.50	0.60	-32.1	0.24	54
440.70	0.69	0.84	-24.6	0.48	54
441.00				0.27	59
442.20	0.46	0.54	-30.6	0.32	50
443.70	0.23	0.28	-32.1	0.22	50
444.10				0.27	59
445.40	0.35	0.46	-32.2	0.26	38
445.60				1.46	155
446.60	0.44	0.47	-30.2	0.24	58
448.00				0.22	59
449.20	0.32	0.38	-31.2	0.20	70
450.20				0.14	42
452.85	0.40	0.45	-33.7	0.17	70
453.80	0.52	0.64	-22.5	0.23	65
456.78				0.21	47
457.58	0.56	0.63	-33.8	0.41	63
458.00				0.52	96
459.66	0.35	0.39	-25.4	0.29	68
461.00				0.45	81
462.50	0.48	0.58	-34.0	0.41	82
464.09	0.52	0.59	-35.0	0.48	100
465.50				0.94	160
467.00	0.67	0.78	-23.1	0.53	92
469.00	0.98	1.13	-35.0	0.55	127
470.50	1.19	1.37	-25.6	1.09	177

*Unpublished results of I. Vető.

**Values can be slightly higher than the true ones since the siderite present in the corresponding samples (see Table 2) starts to decompose at the final temperature of the Rock-Eval pyrolysis and contributes some inorganic carbon to the TOC measurement.

Table 2
Mineralogical composition of samples from the Cs 61 section

Depth (m)	Montm. (%)	Ill./sm. (%)	Illite (%)	Kaolin. (%)	Chlorite (%)	Quartz (%)	K-feld. (%)	Plag. (%)	Calcite (%)	Dolom. (%)	Aragon. (%)	Pyrite (%)	Gypsum (%)	Zeolite (%)	Siderite (%)	Amorph. (%)
400.50	15	7	10		3	20	2	2	27	3	4	3	tr			4
402.00	18	7	10		6	23	2	3	18	4	3	2	tr			4
403.60	13	7	11		3	22	1	2	26	3	4	4	tr			4
405.00	17	9	12		2	24	1	3	19	3	2	3		1		4
407.80	15	7	12	1	2	31	1	6	15	2	1	3	tr			4
409.20	19	10	10	2	1	26		3	15	3	1	3	tr	1		5
410.70	21	9	15		6	20	2	2	13	4		3	tr			5
412.10	19	9	12	2	3	16	2	1	19	7	2	3	tr			5
413.40	20	9	11	2	1	21	tr	4	19	4	1	3	tr			5
415.10		17	14	3	3	28	2	3	18	2	2	4	tr			4
416.60	19	10	10	1	2	28	1	6	14	2	1	2	tr			4
418.20	21	9	12		4	19	1	6	16	3	2	3	tr			4
419.70		17	12	1	3	36	1	5	14	3	tr	3	tr			5
421.20	18	7	11		3	29	1	4	14	4		4	tr			5
425.70	17	10	14		2	29	1	3	13	2	1	4	tr			4
427.00	15	10	12		2	36	1	3	13	2	tr	2	tr			4
428.90		20	14		3	28	1	3	18	1	3	3	tr		2	4
431.70	12	8	**9		3	28	1	1	21	3	4	3		1		6
433.20	15	11	13	2		26	2	5	16	1	2	3	tr			4
434.70	16	10	17		4	21	1	2	15	1	4	2	tr		2	5
436.40	11	10	12	1		6	3	3	38	2	6	3				5
437.90	12	10	8		2	8	2	2	44	1	4	3	tr			4
439.20	13	8	11		2	6	2	2	42	2	5	3	tr			4
440.70	17	10	11		4	18	1	2	25	2	3	3	tr			4
441.00	20	10	10		5	13	2	2	28	1	2	2	tr			5
442.20	21	10	9		5	14	2	2	23	2	3	3	tr			6
442.20	17	9	9		4	11	2	1	37	2	2	2	tr			4
443.70	15	8	11		4	11	2	2	37	2	2	2	tr			4
445.40	17	11	13		2	25	1	3	18	3	1	2	tr			4
446.60	16	8	9		4	12	1	1	39	2	2	2	tr			4
449.20	11	4	5		3	8	1	1	59	*3	1	1				3
450.2	9	6	5		3	4	2	1	62	*3	1	1				3
452.85	12	5	8		3	8	2	2	48	*4	2	2				4
453.80		10	9	4		10	2	1	53	*3	2	2	tr			4
456.78	9	7	12		2	7	2	1	48	*4	2	2	tr			4
457.58	14	8	10		5	10	2	1	34	3	4	3	1	1		4
459.66	11	5	8		3	8	2	1	51	*4	2	1	tr			4
462.50	12	5	6		5	10	2	2	42	7	3	2	tr			4
464.09	9	5	7		3	14	2	1	42	8	3	3	tr			3
467.00	10	4	7		3	19	2	1	37	5	4	4	1			3
469.00	8	3	5		3	32	1	3	29	8	2	3	tr			3
470.50	14	5	10		4	30	2	3	19	4	3	3	tr			3

tr trace amount; *iron rich; **muscovite.

Montm. = montmorillonite; Ill./sm. = illite/smectite; Kaolin. = kaolinite; K-feld. = K-feldspar; Plag. = plagioclase; Dolom. = dolomite; Aragon. = aragonite; Amorph. = amorphous material.

and 470 m) the diversity exhibits higher values (between 2 and 3). In the middle part of the section (around 432 m) a drop in diversity is observed, and the $H(S)$ values show strong fluctuations between 1 and 2.

5.2.2. $P/B+P$

Planktic foraminifera are absent at the base and the top of the section. $P/B+P$ vary between 0% and 34.8%

with continuous fluctuation throughout the section (Appendix A). The maximum value is observed in the upper part of the section at 433.2 m (See Fig. 7).

5.2.3. Q -mode factor analysis

The Q -mode factor analysis shows that the benthic foraminiferal assemblages are characterized by five factor communities (Fig. 7; Table 3), which explain

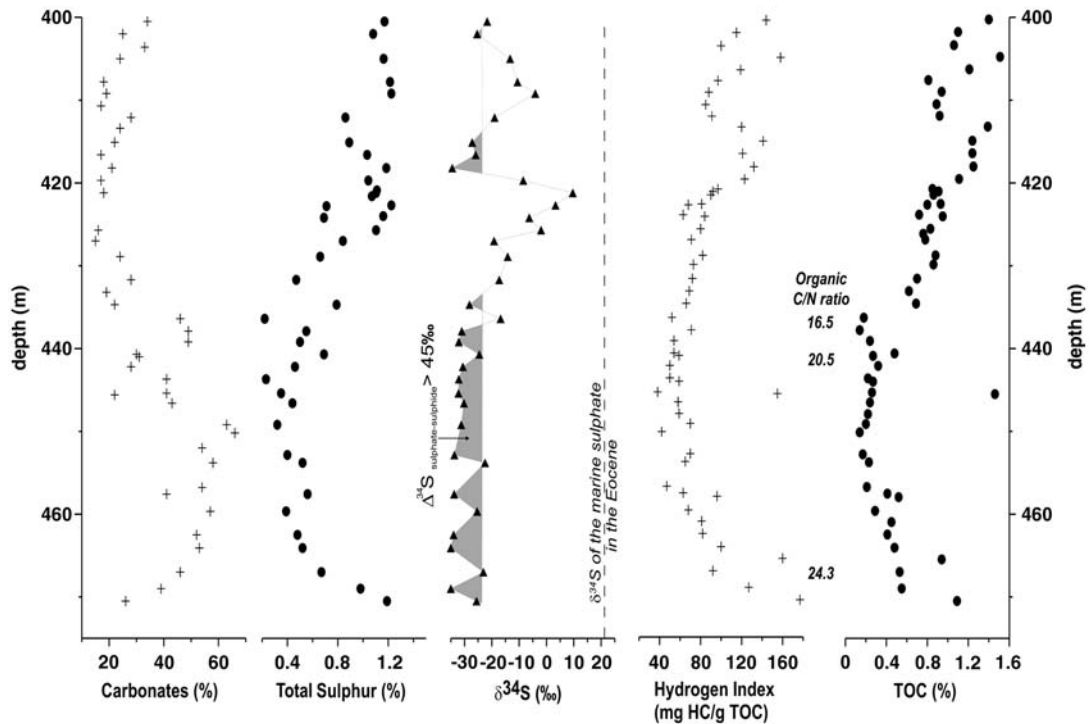


Fig. 6. Variation of carbonate, sulphur, and TOC contents, $\Delta^{34}\text{S}$ and Hydrogen Index vs. depth.

85.7% of the total variance. *Cibicidoides eocaenus* is the dominant species (factor score 6.678) in the factor community 1 (FC-1). Important (i.e. factor score >1) associated species of this fauna include *Cibicidoides perlucidus* and *Heterolepa dutemplei*. This community occurs between 462.5 m and 434.7 m and this fauna is typical in oligotrophic to mesotrophic environment (e.g. Murray, 1991). The FC-2 exhibits statistically significant factor loadings between 433.2 m and 425.7 m and between 418.2 m and 400.5 m. This community explains 22.4% of the total variance and includes only *Bulimina truncana*, which is an infaunal species and represents a decrease in oxygen concentration of bottom water. Significant loadings of the FC-3 occur at the base (between 470.5 m and 458.0 m) and between 421.2 m and 412.1 m. The dominant species is *Lenticulina platyptera* and the important associated species is *Lenticulina arcuatostriata*. The 428.9 m to 416.6 m interval is characterized by FC-4. It explains 4.56% of the total variance and comprises the dominating species *Uvigerina multistriata*, and associated *Uvigerina eocaena*, *C. eocaenus* and *Uvigerina hourcqi*. The FC-5 is restricted to the top of the section (between 405.0 m and 402.0 m). This factor consists of *Bolivina elongata* and *Heterolepa dutemplei* and explains 3.24% of the total variance.

5.2.4. BFOI

A number of studies documented that test morphology of calcareous benthic foraminifers is related to microhabitat preferences (e.g. Corliss, 1985; Corliss and Chen, 1988; Mackensen and Douglas, 1989; Corliss, 1991; Jorissen et al., 1995) which is strongly controlled by organic carbon flux rates, together with dissolved oxygen content at the sediment–water interface and the uppermost few centimeters of the sediment (e.g. Mackensen et al., 1985; Schmiedl et al., 1997). On the basis of this concept the infaunal and epifaunal species groups can be unequivocally distinguished. Epifaunal species, living on the sediment or in the uppermost centimeter of the sediment include planconvex or trochospirally coiled species with thick wall and generally large size. Infaunal species living below the surface of sediment, are cylindrical, rectilinear or oval with thin elongate, flattened wall. Generally, under oligotrophic condition the foraminifers abundance and diversity are rather low and the fauna mainly contains epifaunal species. Under mesotrophic conditions the species abundance and diversity reaches a maximum. The benthic foraminifers assemblages contain epifaunal and shallow or deep infaunal species. Under eutrophic conditions, where the oxygen content decreases to critical level, a low-diversity benthic foraminifers fauna

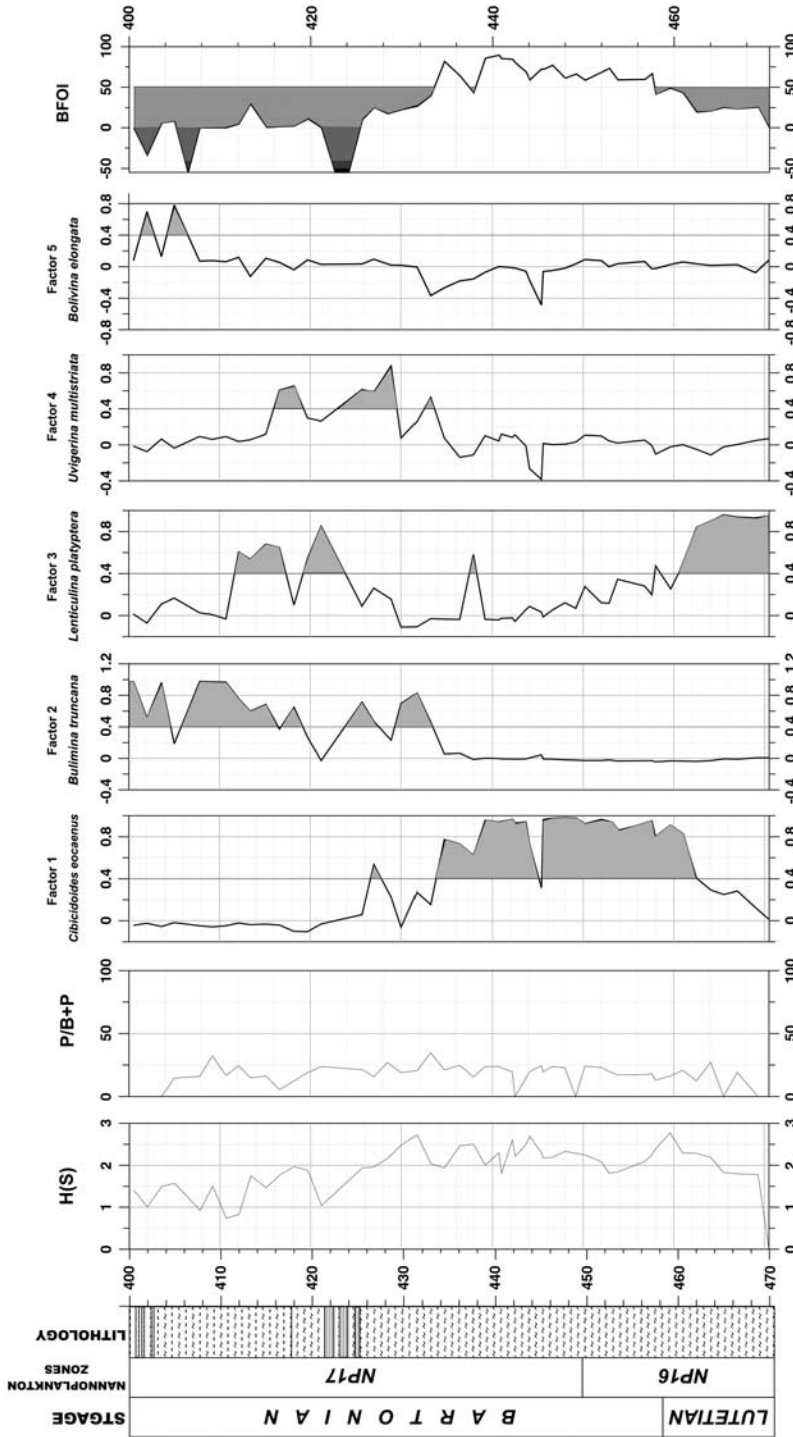


Fig. 7. Diversity $H(S)$, Plankton/Benthos ratio ($P/P+B$), Q-mode (Varimax-rotated) factor analysis and Benthic Foraminiferal Oxygen Index (BFOI) vs. depth in Cs 61 section.

Table 3
Factor scores of dominant and associated species from Cs 61 section

Factors	Dominant species	Factor scores	Associated species	Factor scores	Explained variance (%)
Factor 1	<i>Cibicidoides eocaenus</i>	6.68	<i>Cibicidoides perlucidus</i> <i>Heterolepa dutemplei</i>	1.28 1.05	41.96
Factor 2	<i>Bulimina truncana</i>	7.13			22.40
Factor 3	<i>Lenticulina platyptera</i>	6.91	<i>Lenticulina arcuatostrata</i>	1.26	13.57
Factor 4	<i>Uvigerina multistriata</i>	4.78	<i>Uvigerina eocaena</i> <i>Cibicidoides eocaenus</i> <i>Uvigerina hourcqi</i>	3.77 1.56 1.10	4.56
Factor 5	<i>Bolivina elongata</i>	4.81	<i>Heterolepa dutemplei</i>	3.10	3.24
					Sum 85.72

develops that mainly contains deep infaunal species (Jorissen et al., 1995).

The estimation of trophic condition in the investigated section is based on the direct palaeoecological information of Eocene and Oligocene taxa according to Kaiho (1991), Kaiho et al. (2006), Oberhänsli et al. (1991), Scherbacher et al. (2001) and Schmiiedl et al. (2002). For those Eocene benthic foraminifers species which have no direct palaeoecological information we inferred their microhabitat preferences from their morphological characteristics according to Corliss (1985, 1991), Corliss and Chen (1988) and Kaiho (1994, 1999).

The zero value of BFOI suggests that low oxic or even suboxic conditions (O_2 concentration ranging between 0.3 and 1.5 ml/l) prevailed during deposition of the lowermost part of the section (at around 470.5 m). BFOI shows a significant upward increase from 470.5 to 440 m, followed by a similarly significant decrease up to 400.5 m (Fig. 7). The BFOI ranges between 15 and 50 in the 469 to 456.8 m interval, indicating low oxic depositional environment (O_2 concentration ranging between 1.5 to 3.0 ml/l). This interval is characterized by the *Lenticulina platyptera* fauna (FC-3) which comprise mainly infaunal species. A comparison with test morphologies of Recent species indicates mesotrophic environment (Corliss and Chen, 1988). Inferred from BFOI values higher than 50, O_2 concentration of the bottom water was above 3.0 ml/l during deposition of the middle part of the section (456.8 to 433.2 m). The *Cibicidoides eocaenus* fauna (FC-1) comprises mainly epifaunal species (e. g. *Cibicidoides perlucidus*, *Heterolepa dutemplei*) and represents an increase in water

depth and oligotrophic environment. Above the middle part of the investigated section the benthic foraminifers fauna comprises mainly shallow and deep infaunal species (e.g. *Bulimina truncana*, *Uvigerina multistriata*, *Bolivina elongata*). Therefore, these assemblages indicate mesotrophic to eutrophic conditions (Corliss, 1985, 1991). These infaunal taxa usually occur along oxygen minimum zones in high productivity areas in recent oceanic environment (Corliss, 1985). Very similar palaeoenvironment is described by Scherbacher et al. (2001) from the Early Oligocene sections of Inneralpine Molasse Basin. They suggest that the depositional system was controlled by high organic carbon fluxes with increasing water depth in a marginal sea.

The BFOI values varying between 50 and 0 indicate approximately between 0.3 and 1.5 ml/l dissolved oxygen content during deposition of the intervals between 433.2 m to 425.7 m. BFOI values ranging between –55 and 0 point to anoxic to low oxic conditions during deposition of 425.7 and 400.5 interval (Fig. 7). The fine lamination observed in the interval 425.6 to 420.6 m supports this assumption.

6. Discussion

6.1. Estimation of C_{flux}

Before addressing calculation of TOC_{or} and SR and attempting estimation of C_{flux} , it is useful to analyse the conditions of sulphate reduction.

6.1.1. Conditions of bacterial sulphate reduction

21.8‰, reported by Kampschulte and Strauss (2004) as the average $\delta^{34}S$ value for oceanic sulphate prevailing in the 30 to 50 Ma BP time interval is considered here as the parent sulphate $\delta^{34}S$ for the late Middle Eocene–Late Eocene sediments of the Cs 61 section. On the basis of this assumption, $\Delta^{34}S_{sulphate-sulphide}$ varies between 12 to 57‰.

The minimum $\Delta^{34}S_{sulphate-sulphide}$ values (as low as 12‰) are observed in the laminated interval. In the relatively closed environment both the original sulphate content of the porewater and the sulphate which entered the sediment by downward diffusion were reduced by bacteria, H_2S was able to escape only by diffusion and the bulk of the sulphide was fixed as S_{red} . It is not surprising that these conditions, close to those characterizing Rayleigh-type fractionation, favored low net sulphur isotope fractionation.

On the other hand, values above 45‰, the maximum depletion in ^{34}S observed in pure bacterial cultures (Kaplan and Rittenberg, 1964) characterize the interval

below 435 m. Here a significant part of the sulphate was probably introduced by bioturbation and in the relatively open environment the greater part of the sulphide produced was not fixed in the sediment and reactions of the oxidative part of the sulphur cycle (i.e. disproportionation of elemental sulphur, sulphite and thiosulphate included, see Section 4.2) were intense. Since disproportionation of these intermediate products are accompanied by strong sulphur isotope fractionation (see Section 4.3), the high depletion in ^{34}S observed in this interval, is not surprising. Samples taken from between 458.5–435.5 m are low in sulphur (TS is below 0.6% in all but one sample, Table 1, Fig. 6), what can be at least partly explained by relatively intense aerobic degradation.

Similarly high values of $\Delta^{34}\text{S}_{\text{sulphate-sulphide}}$ have been found in some organic-rich samples of the uppermost 20 m of the section. According to previous interpretations (Beier and Hayes, 1989), coupling of strong sulphur isotope fractionation and organic-rich sediments indicates significant contribution of pyrite precipitated in a sulphidic water column. Recent finding of this coupling in organically rich sediments deposited under dysoxic water (Brüchert et al., 2000) proves that there is no need to invoke sulphidic waters to explain very negative $\delta^{34}\text{S}$ of S_{red} in such sediments.

6.1.2. Variation of mass accumulation rate

A combined bio- and magnetostratigraphic study of the Eocene strata penetrated by the nearby Csetény 72 (Cs 72) borehole (see Fig. 1B) permitted to calculate average sedimentation rates (SR) for the time period corresponding the NP16 and NP17 biozones (Kollányi et al., 2003). Considering the less than 1 km distance separating the two well sites (Fig. 1B), the average SR values obtained by these authors for the Cs 72 Eocene section are expected to be valid also for the Cs 61 core. The correlation of the two cores is based on the NP16–NP17 boundary, well defined in both of them, which coincides with the base of the C18 normal polarity magnetic zone in the Cs 72 core (Fig. 8).

Based on this correlation, the studied section is divided into 3 intervals (Fig. 8). Interval A (470.5–447 m) covers the bulk of the C18 reversed polarity magnetic zone, interval B represents the C18 normal polarity magnetic zone, and interval C (425.2–400.5 m) encompasses the C17 reversed polarity magnetic zone and the lower half of the C17 normal polarity magnetic zone. With some simplifications we assume that intervals A and C are characterized by the same average SR values as are the entire 478.2–447 and 425.2–384 m intervals, respectively. Average SR values are displayed on Fig. 8.

It is obvious that average SR can be very different from the actual SR values of individual samples. Variation of mineralogical composition is expected to shed some light on the variation of SR within the three intervals. The bulk of the studied sediments consists of a mixture of three mineral groups: syngenetic carbonates (calcite+aragonite), clay minerals and quartz+feldspar. The second and third groups are either of terrestrial origin or derived from pyroclastic material. It is easy to understand that a significant change in SR should be accompanied by changes in the relative weight of at least two of these mineral groups.

Interval A is characterized by a strong upward increase of syngenetic carbonate, strong upward decrease of the quartz+feldspar content and a high scatter with no depth trend of the clay mineral content (Fig. 9). At the boundary of intervals A and B, clay minerals and syngenetic carbonates show a pronounced rise and drop, respectively. Contrasting with progressive changes in mineralogical composition throughout interval A, interval B is clearly divided into two parts of distinctly different mineralogies by a second major drop of syngenetic carbonates and significant rise of quartz+feldspar: its lower half (interval B₁) is low in quartz+feldspar and is characterized by high amounts and high scatter of syngenetic carbonates compared to its upper half (interval B₂) (Fig. 9). Clay minerals show high scatter in both intervals and no one of the three mineral groups shows clear depth trend in intervals B₁ and B₂. Finally, mineralogical composition of interval C is similar to that of the interval B₂. This pattern is tentatively explained as follows.

During deposition of interval A, the water depth progressively increased and the shoreline moved away from the Cs 61 site. Consequently, less and less terrigenous material reached the site and the fine-grained clay minerals become progressively enriched relative to quartz+feldspar. This scenario resulted in a decrease of SR, which is indicated by the dashed line of Fig. 9; but this line is not considered to reflect the change in SR quantitatively.

The major fall of syngenetic carbonates and rise of clay minerals at the boundary between intervals A and B₁, characterized by very different average SR values, is at least partly explained by a sudden decrease of the SR and a sudden slowing down of carbonate accumulation. Absence of clear depth trends in interval B₁ suggests that the SR remained relatively constant during the corresponding time period.

The pronounced drop of syngenetic carbonates and the important rise of quartz+feldspar, observed at the boundary between intervals B₁ and B₂, suggest a second sudden change in SR.

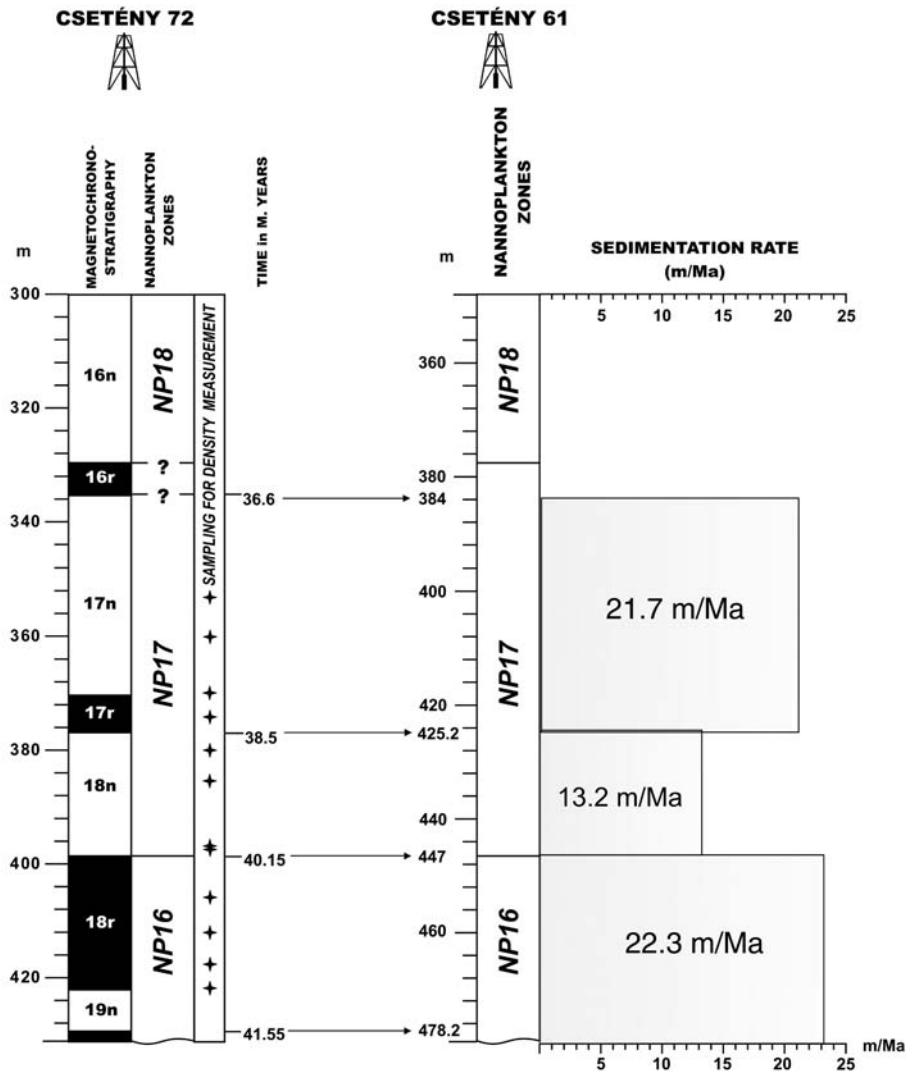


Fig. 8. Stratigraphical correlation between the Eocene sequences of Cs 72 and Cs 61 boreholes.

Due to their mineralogical similarity, intervals B₂ and C are considered here to have identical average SR.

The corresponding average SR values of the four intervals are listed in Table 4 and displayed on the right side of Fig. 9. While the average SR can be very different of the true SR in case of interval A (as it is illustrated by the dashed line on Fig. 9) and B₁, it is considered not to differ fundamentally from the true SR in case of the other two intervals.

For estimation of C_{flux} mass accumulation rate (MAR) has to be used instead of SR. MAR is calculated by multiplying SR by the dry density (ρ). Since ρ has not been measured directly in the section, its values measured on core samples taken from the Eocene section of the nearby Cs 72 hole (KBFI, 1992) are used.

Sampling points are indicated on Fig. 8 and average ρ and MAR values are listed in Table 4.

6.1.3. Original amount of organic carbon

The low T_{max} values (see Section 5.1) suggest that the OM is immature, hence there is no need to take into account any thermal loss of organic carbon in the TOC_{or} calculation.

In the first step ΔTOC_{sulf} has been estimated by replacing S_{red} and $\Delta^{34}S_{sulphate-sulphide}$ in Eq. (8) with TS values listed in Table 1, and $\Delta^{34}S_{sulphate-sulphide}$ values calculated using 21.8‰ for parent sulphate $\delta^{34}S$ (see Section 6.1.1), respectively. The obtained ΔTOC_{sulf} values together with corresponding TOC values are displayed on Fig. 10.

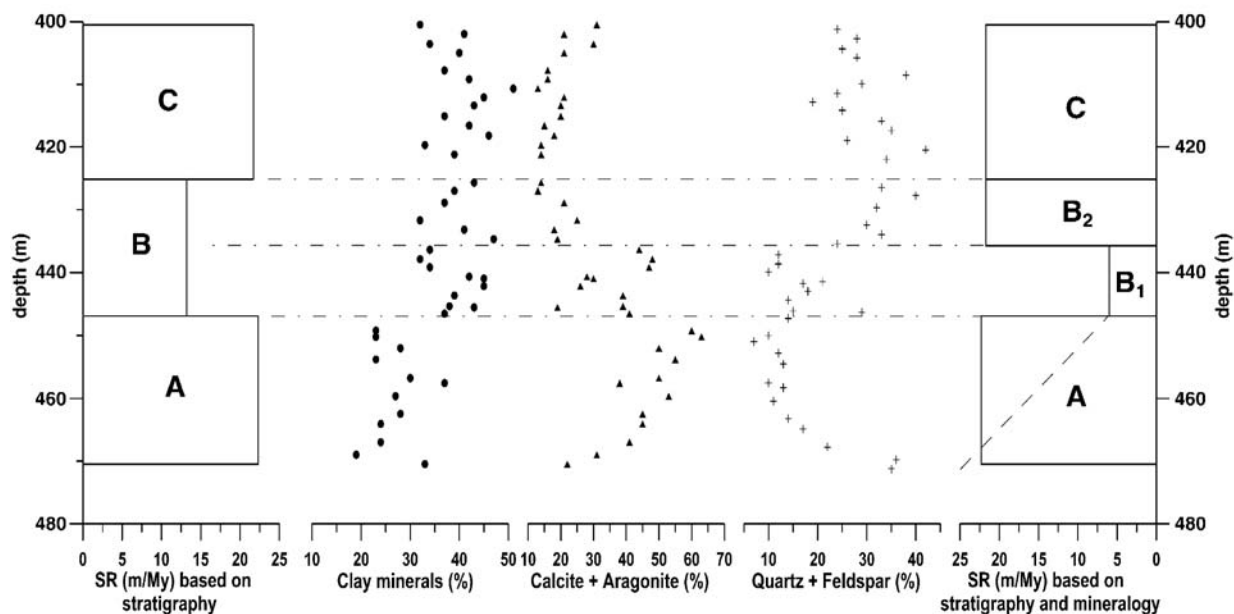


Fig. 9. Variation of clay minerals, calcite+aragonite and quartz+feldspar contents along depth with average MAR values.

In two laminated samples (421.2 and 422.7 m) $\Delta^{34}\text{S}_{\text{sulphate-sulphide}}$ is so low that $\Delta\text{H}_2\text{S}$ would be negative (see Eq. (7)) and Eq. (8) would not give a meaningful result. Therefore $\Delta\text{TOC}_{\text{sulf}}$ is estimated for these samples using Eq. (4) where $\Delta\text{H}_2\text{S}$ is replaced with zero. Consequently, the corresponding $\Delta\text{TOC}_{\text{sulf}}$ values are minimum ones.

$\Delta^{34}\text{S}_{\text{sulphate-sulphide}}$ is higher than 45‰ for some samples taken from the uppermost 20 m and for most of the samples studied from below 435.5 m. In such case Eq. (8) could significantly overestimate $\Delta\text{TOC}_{\text{sulf}}$ (see Section 4.2), therefore $\Delta^{34}\text{S}_{\text{sulphate-sulphide}}$ has been replaced with 45‰ for these samples. Consequently, the corresponding $\Delta\text{TOC}_{\text{sulf}}$ values are minimum ones. Samples from below 460 m have been deposited in the photic zone (Fig. 11), consequently Eq. (8) cannot be used for estimating the corresponding $\Delta\text{TOC}_{\text{sulf}}$ values. Consequently the $\Delta\text{TOC}_{\text{sulf}}$ curve starts only at 460 m (Fig. 10). Average $\Delta\text{TOC}_{\text{sulf}}$ values characterizing the four intervals are listed in Table 5 and displayed on Fig. 10.

In the second step estimation of $\Delta\text{TOC}_{\text{aer}}$ has been attempted. Since MAR and bottom water O_2 content are the two main variables controlling the relative weight of aerobic oxidation of OM (see Section 4.2), estimation of $\Delta\text{TOC}_{\text{aer}}$ has been attempted differently for interval C and intervals B₂, B₁ and A.

Sediments of interval C were deposited under relatively oxygen-depleted bottom water; on the basis of BFOI values, its O_2 content varied mostly between 0 and 1.8 ml/l and the development of fine lamination

below 420.6 m suggests that O_2 content was below 0.2 ml/l during the corresponding time interval (Table 5). On the other hand, the average MAR characterizing the interval C is 49 g/m²/y (Table 4).

According to Kristensen et al. (1999), the bottom water O_2 content and MAR prevailing on a shelf and slope transect off the Pacific coast of Mexico vary between 0.1 to 0.4 ml/l and 150 to 70 g/m²/y, respectively. Aerobic respiration roughly accounts for at least 5–28% of the 0–30 cm integrated carbon mineralisation at their studied transect off Mexico. Since sulphate reduction is intense below 30 cm, the true relative weights of the aerobic respiration cannot be higher than 5–28%. These values correspond to $\Delta\text{TOC}_{\text{aer}}/\Delta\text{TOC}_{\text{anaer}}$ ratios varying between 0.05 to 0.4.

With cautions, the results of Kristensen et al. (1999) can be used for estimating $\Delta\text{TOC}_{\text{aer}}$ in the interval C. While the range of the local bottom water O_2 content prevailing during its deposition overlaps the range of that measured at the transect off Mexico, the corresponding

Table 4
Variation of sedimentation rate (SR), density (ρ) and mass accumulation rate (MAR) along the Cs 61 section

Depth (m–m)	Interval	Average SR (m/My)	ρ (g/cm ³)	Average MAR (g/m ² /y)
400.5–425.2	C	21.7	2.26 (4)	49
425.2–435.5	B ₂	21.7	2.17 (2)	47
435.5–447.0	B ₁	6.0	2.31 (2)	14
447.0–470.5	A	22.3	2.44 (4)	54

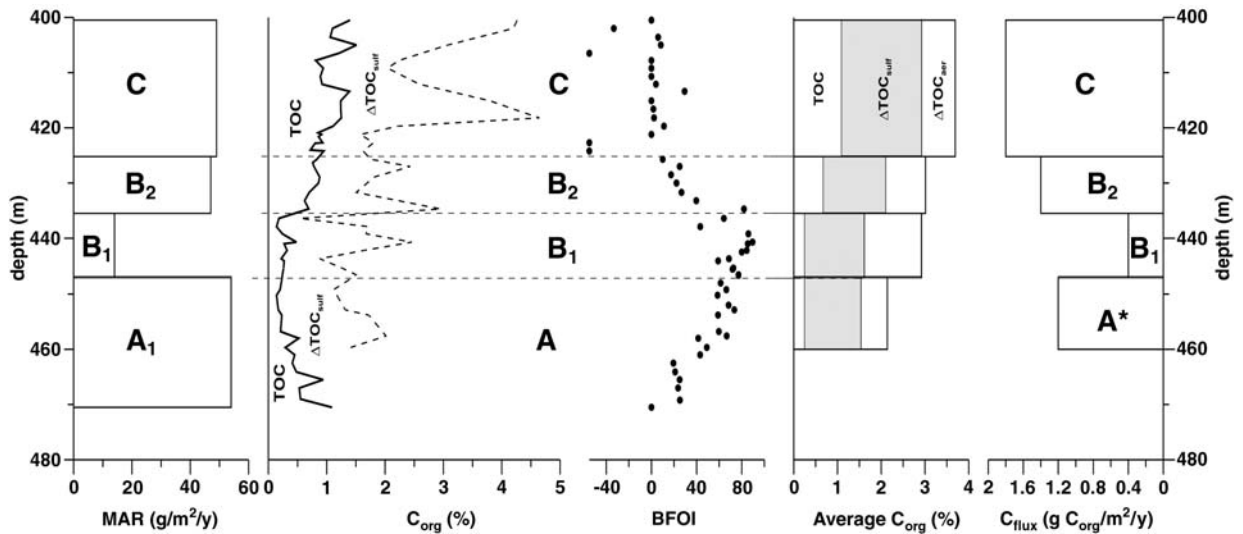


Fig. 10. Variations of TOC_{or}, BFOI, average MAR values and proposed evolution of C_{flux}. Interval A* represents only a part of interval A; the sediments of the lowest 10 m of the section were deposited in photic conditions, consequently C_{flux} cannot be estimated for them (see Section 6.1.3).

sediments deposited more slowly than the sediments of the transect off Mexico (Table 5). Therefore 0.4, the highest $\Delta\text{TOC}_{\text{aer}}/\Delta\text{TOC}_{\text{anaer}}$ ratio observed there, seems to be a reasonable value to be used in calculation of $\Delta\text{TOC}_{\text{aer}}$ for interval C. The obtained $\Delta\text{TOC}_{\text{aer}}$ and TOC_{or} values are listed in Table 5. and displayed on Fig. 10.

Choosing appropriate $\Delta\text{TOC}_{\text{aer}}/\Delta\text{TOC}_{\text{anaer}}$ ratios for intervals B₂, B₁ and A seems to be a more difficult exercise. In view of variation of BFOI along depth,

bottom water O₂ content progressively increased from 1.5 to >3.5 ml/l during deposition of interval A and the lower half of the interval B₁ then it progressively decreased up to 1.7 ml/l during deposition of the upper half of the interval B₁ and the interval B₂. On other hand, the MAR progressively decreased during deposition of interval A (see the dashed line on Fig. 10) then was very low in the time period corresponding to interval B₁, and finally, was high thereafter during deposition of interval B₂.

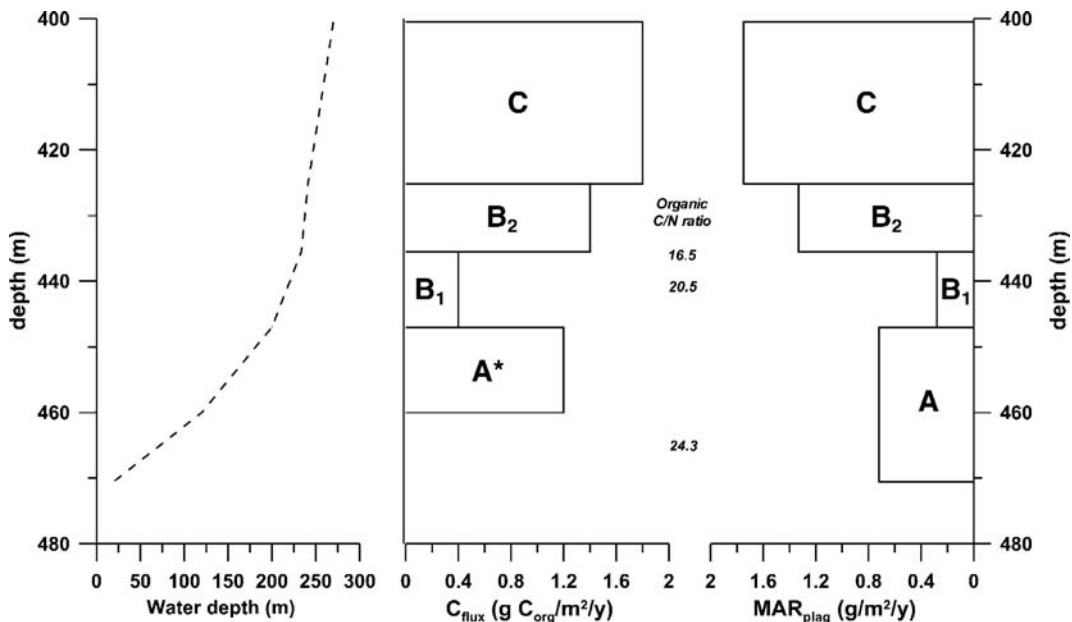


Fig. 11. Proposed evolution of C_{flux}, evolution of water depth and average MAR_{plag}. The water depth is estimated after Báldi-Beke and Báldi (1991).

Table 5

Variation of mass accumulation rate (MAR), bottom water O₂ content, TOC, $\Delta\text{TOC}_{\text{sulf}}$, $\Delta\text{TOC}_{\text{aer}}$, TOC_{or} and C_{flux} along the Cs 61 section with MAR and bottom water O₂ content measured at an off Mexico transect (data from Kristensen et al., 1999)

Depth (m–m)	Interval/transect	Average MAR (g/m ² /y)	O ₂ content (ml/l)	TOC (%)	$\Delta\text{TOC}_{\text{sulf}}$ (%)	$\Delta\text{TOC}_{\text{aer}}$ (%)	TOC_{or} (%)	C_{flux} (g C or /m ² /y)
400.5–425.2	C	49	0–1.8	1.1	1.85	0.74	3.69	1.81
425.2–435.5	B ₂	47	1.7–2.7	0.8	1.31	0.92	3.01	1.41
435.5–447.0	B ₁	14	2.5–6	0.3	1.33	1.33	2.92	0.41
447.0–470.5	A	54	1.5–3	0.3	1.26	0.62	2.14	1.16
	Off Mexico	70–150	0.1–0.4					

This evolution of MAR and bottom water O₂ content resulted in a progressive increase of the $\Delta\text{TOC}_{\text{aer}}/\Delta\text{TOC}_{\text{anaer}}$ ratio during the time period represented by interval A and the bottom of the interval B₁ and its progressive decrease during deposition of the top of the interval B₁ and the interval B₂, while $\Delta\text{TOC}_{\text{aer}}/\Delta\text{TOC}_{\text{anaer}}$ ratio was likely the highest and remained relatively constant during deposition of the middle of the interval B₁, characterized by the highest bottom water O₂ content and low MAR.

Therefore the following more or less arbitrary approach has been applied for estimation of $\Delta\text{TOC}_{\text{aer}}$: the $\Delta\text{TOC}_{\text{aer}}/\Delta\text{TOC}_{\text{anaer}}$ ratio has been replaced with 1 for interval B₁ since $\Delta\text{TOC}_{\text{aer}}$ is seldom greater than $\Delta\text{TOC}_{\text{sulf}}$ in continental margin sediments (Canfield, 1994) while it was replaced with 0.7 for intervals A and B₂. By multiplying average $\Delta\text{TOC}_{\text{sulf}}$ values with the corresponding $\Delta\text{TOC}_{\text{aer}}/\Delta\text{TOC}_{\text{anaer}}$ ratios, $\Delta\text{TOC}_{\text{aer}}$ values have been obtained for the four intervals (Table 5, Fig. 10).

$\Delta\text{TOC}_{\text{or}}$ values have been obtained for the four intervals by summarising TOC, $\Delta\text{TOC}_{\text{sulf}}$, and $\Delta\text{TOC}_{\text{aer}}$ (Table 5, Fig. 10). $\Delta\text{TOC}_{\text{or}}$ shows a progressive upward increase throughout the section.

6.1.4. Uncertainties and errors

In view of the novelty of the estimation applied, it is necessary to overview the sources of uncertainty and error together their relative importances.

6.1.4.1. Estimation of $\Delta\text{TOC}_{\text{sulf}}$ First the uncertainties of the variables used in Eq. (8) and those inherent to the equation itself are analysed.

The uncertainty of S_{red} is the accuracy of TS measurement, $\pm 10\%$. Uncertainties of TS are listed in Table 6.

The uncertainty introduced by $\Delta^{34}\text{S}_{\text{sulphate-sulphide}}$ is at least $\pm 1.2\%$, the sum of accuracy of the $\delta^{34}\text{S}$ measurement used and the standard deviation of $\delta^{34}\text{S}$, given by Kampschulte and Strauss (2004) for average S-isotope composition of Eocene seawater sulphate. If

$\Delta^{34}\text{S}_{\text{sulphate-sulphide}}$ is replaced with $(\Delta^{34}\text{S}_{\text{sulphate-sulphide}} \pm 1.2\%)$ in Eq. (8), the resulting change of $\Delta\text{TOC}_{\text{sulf}}$ changes from ± 3 to $\pm 12\%$ when $\Delta^{34}\text{S}_{\text{sulphate-sulphide}}$ increases from 20 to 45‰.

Since R^2 characterizing Eq. (7) is 0.919 (Fig. 5), the equation itself introduces about $\pm 8\%$ uncertainty in estimation of $\Delta\text{TOC}_{\text{sulf}}$.

Canfield and Teske (1996) studied the relationship between $\Delta\text{H}_2\text{S}$ and net S-isotope fractionation only for pyrite + acid-volatile sulphide phases while in this work the whole S_{red} , S_{org} included has been measured and considered. For the purpose of this work it is appropriate to take into consideration S_{org} , too. On the other hand, S_{org} is enriched in ^{34}S relative to co-existing pyrite in most sedimentary rocks by an average of about 10‰ (Anderson and Pratt, 1995). The balance between disadvantage and benefit caused by taking into consideration S_{org} is difficult to assess, but in view of small amounts of this sulphur species (see Table 6), this problem is not really important in case of Cs 61 section.

Up to now the presence of sulphatic sulphur (S_{SO_4}) – both baritic and structurally substituted in carbonates – has been neglected in estimation of $\Delta\text{TOC}_{\text{sulf}}$ in the Cs 61 samples. Due to presence of S_{SO_4} , TS is $> S_{\text{red}}$, hence $\Delta\text{TOC}_{\text{sulf}}$ is overestimated.

Amounts of S_{SO_4} are assessed from amounts of syngenetic carbonates and BaO, supposing that Ba present in the samples is entirely fixed in barite, as follows:

$$\text{S}_{\text{SO}_4} = (\text{calcite} + \text{aragonite}) \times 0.0436 / 100 + 0.209 \times \text{BaO} \quad (9)$$

where S_{SO_4} , calcite, aragonite, and BaO are expressed in %, 0.0436 is the average concentration of lattice bound sulphur in bulk carbonate expressed in %, as reported by Burdett et al. (1989) for 12 recent marine sediment samples, and 0.209 is the weight ratio of sulphur and BaO in barite. Calculated S_{SO_4} contents listed in Table 6 are in all but one case smaller than the uncertainties of TS, hence the overestimation of $\Delta\text{TOC}_{\text{sulf}}$ caused by presence of this sulphur species is negligible.

Table 6

Variation of calcite, aragonite, BaO, TS, TOC contents, $\delta^{34}\text{S}$, uncertainty of TS (TS_{unc}) with calculated S_{SO_4} , S_{org} , $\delta^{34}\text{S}_{\text{red}}$ values along the Cs 61 section

Depth (m)	Calcite (%)	Aragonite (%)	BaO (%)	$\text{S}_{\text{SO}_4}^*$ (%)	TS_{unc} ($\pm\%$)	TS (%)	S_{org}^* (%)	$\delta^{34}\text{S}$ (‰)	$\delta^{34}\text{S}_{\text{red}}^*$ (‰)	TOC (%)
400.50	27	4	0.03	0.02	0.12	1.17	0.05	-21.7	-22.4	1.40
402.00	18	3	0.03	0.02	0.11	1.08	0.04	-25.4	-26.1	1.10
405.00	19	2	0.03	0.02	0.12	1.16	0.05	-13.3	-13.8	1.51
407.80	15	1	0.03	0.01	0.12	1.21	0.03	-10.6	-11.0	0.81
409.20	15	1	0.03	0.01	0.12	1.22	0.03	-4.1	-4.4	0.94
412.10	19	2	0.03	0.02	0.09	0.86	0.03	-19.0	-19.7	0.92
415.10	18	2	0.03	0.02	0.09	0.89	0.04	-27.2	-28.1	1.24
416.60	14	1	0.04	0.01	0.10	1.03	0.04	-25.9	-26.6	1.24
418.20	16	2	0.04	0.02	0.12	1.18	0.04	-34.5	-35.2	1.25
419.70	14	tr	0.03	0.01	0.10	1.04	0.04	-8.5	-8.9	1.11
421.20	14	–	0.04	0.02	0.11	1.10	0.03	9.6	9.4	0.91
422.70	nd	nd	0.04	nc	0.12	1.22	0.03	3.3	nc	0.93
424.20	nd	nd	0.04	nc	0.07	0.69	0.03	-6.3	nc	0.95
425.70	13	1	0.04	0.01	0.11	1.10	0.03	-2.0	-2.3	0.83
427.00	13	tr	0.04	0.01	0.08	0.84	0.03	-19.2	-19.9	0.78
428.90	18	3	0.04	0.02	0.07	0.66	0.03	-14.2	-15.2	0.88
431.70	21	4	0.03	0.02	0.05	0.47	0.03	-17.3	-18.8	0.70
434.70	15	4	0.03	0.02	0.08	0.79	0.02	-28.2	-29.2	0.69
436.40	38	6	0.02	0.02	0.02	0.22	0.01	-16.8	-21.3	0.18
437.90	44	4	0.01	0.02	0.06	0.55	0.01	-31.0	-33.4	0.14
439.20	42	5	0.01	0.02	0.05	0.50	0.01	-32.1	-34.7	0.24
440.70	25	3	0.03	0.02	0.07	0.69	0.02	-24.6	-25.8	0.48
442.20	23	3	0.02	0.02	0.05	0.46	0.01	-30.6	-32.5	0.32
443.70	37	2	0.02	0.02	0.02	0.23	0.01	-32.1	-37.6	0.22
445.40	37	2	0.02	0.02	0.04	0.35	0.01	-32.2	-35.7	0.26
446.60	39	2	0.02	0.02	0.04	0.44	0.01	-30.2	-32.8	0.24
449.20	59	1	0.01	0.03	0.03	0.32	0.01	-31.2	-36.4	0.20
452.85	48	2	0.02	0.03	0.04	0.40	0.01	-33.7	-37.6	0.17
453.80	53	2	0.02	0.03	0.05	0.52	0.01	-22.5	-25.0	0.23
457.58	34	4	0.02	0.02	0.06	0.56	0.01	-33.8	-35.9	0.41
459.66	51	2	0.02	0.03	0.04	0.39	0.01	-25.4	-28.8	0.29

tr traces; nd not determined; nc no calculated; *calculated data.

The heavy isotope composition of S_{SO_4} , identical of that of the sulphate dissolved in the depositing sea (Kampschulte and Strauss, 2004) is an additional source of error. The relationship between isotope compositions and amounts of TS and S_{red} is expressed as follows:

$$\delta^{34}\text{S} = (\delta^{34}\text{S}_{\text{red}} \times \text{S}_{\text{red}} + 21.8 \times \text{S}_{\text{SO}_4}) / \text{TS} \quad (10)$$

where $\delta^{34}\text{S}_{\text{red}}$ is the sulphur isotope composition of S_{red} and 21.8 is the average S-isotope composition of Eocene seawater sulphate, both expressed in ‰. Obtained $\delta^{34}\text{S}_{\text{red}}$ values are listed in Table 6. Difference between $\delta^{34}\text{S}$ and $\delta^{34}\text{S}_{\text{red}}$ is smaller than 1.2‰, the uncertainty of $\Delta^{34}\text{S}_{\text{sulphate-sulphide}}$ in case of samples taken from intervals B₂ and C. On the contrary, this difference is greater than 1.2‰ in case of samples taken from intervals B₁ and A. Consequently, the heavy isotope composition of S_{SO_4} causes underestimation in case of these intervals.

If $\Delta^{34}\text{S}_{\text{sulphate-sulphide}}$ is greater than 45‰, it is replaced with 45‰, in Eq. (8), hence the corresponding $\Delta\text{TOC}_{\text{sulf}}$ is underestimated.

6.1.4.2. Estimation of $\Delta\text{TOC}_{\text{aer}}$ $\Delta\text{TOC}_{\text{aer}}$ has been defined as the product of $\Delta\text{TOC}_{\text{sulf}}$ and the $\Delta\text{TOC}_{\text{aer}}/\Delta\text{TOC}_{\text{sulf}}$ ratio. Consequently, this step of estimation propagates the uncertainty and error introduced in estimation of $\Delta\text{TOC}_{\text{sulf}}$. Uncertainty and error introduced by the choice of the numerical values of $\Delta\text{TOC}_{\text{aer}}/\Delta\text{TOC}_{\text{sulf}}$ ratio obviously cannot be numerically expressed.

6.1.4.3. Uncertainty and error in estimation along the section. Table 7 summarises uncertainties and errors introduced in the two steps of estimation separately for the 4 intervals.

Uncertainties introduced by TS and the Eq. (8) are 10 and $\pm 8\%$, respectively, throughout the entire Cs 61 section.

Table 7

Uncertainties and errors in TOC_{or} estimation along the Cs 61 section

	$\Delta\text{TOC}_{\text{sulf}}$		Error	$\Delta\text{TOC}_{\text{aer}}$		TOC_{or} (%)
	Uncertainty			Uncertainty		
	($\pm\%$)	($\pm C_{\text{org}}\%$)		($\pm\%$)	($\pm C_{\text{org}}\%$)	
C	28	0.52	Slight underestimation	>28	>0.21	3.69
B ₂	28	0.37	–	>28	>0.26	3.01
B ₁	>33	>0.44	Underestimation	$\gg 33$	$\gg 0.44$	2.92
A	>33	>0.42	Underestimation	$\gg 33$	$\gg 0.20$	2.14

On the contrary, that introduced by $\Delta^{34}\text{S}_{\text{sulphate-sulphide}}$ changes from ± 3 to $\pm 12\%$ as $\Delta^{34}\text{S}_{\text{sulphate-sulphide}}$ increases from 20.26 to 45‰. $\Delta^{34}\text{S}_{\text{sulphate-sulphide}}$ is replaced with 45‰ for all but one samples studied from intervals A and B₁, while it varies between 20.26 and 45‰ for the majority of the samples studied from intervals B₂ and C. Because of this difference average uncertainty introduced by $\Delta^{34}\text{S}_{\text{sulphate-sulphide}}$ is ± 7.5 and $\pm 12\%$ for the upper and lower intervals, respectively. This difference is reflected in total uncertainties introduced in both steps of estimation.

Since $\Delta^{34}\text{S}_{\text{sulphate-sulphide}}$ is greater than 45‰ for the great majority of the samples belonging to A and B₁ intervals, the corresponding $\Delta\text{TOC}_{\text{sulf}}$ values are underestimated. The relative importance of the isotopically heavy S_{SO_4} in TS in the above intervals is an additional source of underestimation. On the contrary, $\Delta^{34}\text{S}_{\text{sulphate-sulphide}}$ is greater than 45‰ for only a minority of the samples belonging to B₂ and C intervals, hence underestimation remains small in that case.

Uncertainties of $\Delta\text{TOC}_{\text{sulf}}$ are propagated and strengthened in estimation of $\Delta\text{TOC}_{\text{aer}}$. At the end of this exercise $\Delta\text{TOC}_{\text{sulf}}$ and $\Delta\text{TOC}_{\text{aer}}$ characterizing intervals B₂ and C seem to be more relevant than those characterizing intervals A and B₁. Since the relative weight of TOC in TOC_{or} is greater in case of upper intervals than in that of the lower ones (Fig 10), TOC_{or} seems to be more relevant for intervals C and B₂, than for intervals B₁ and A.

6.1.5. Evolution of the C_{flux} and its interpretation

C_{flux} is the product of TOC_{or} and MAR as shown in the following equation

$$C_{\text{flux}} = \text{TOC}_{\text{or}} \times \text{MAR} \quad (11)$$

where C_{flux} , TOC_{or} and MAR are expressed in $\text{g } C_{\text{org}}/\text{m}^2/\text{y}$, mg/g and $\text{g/m}^2/\text{y}$, respectively. Values of MAR and TOC_{or} , displayed on Fig. 10 and listed in Table 5 are fed into Eq. (11). The obtained C_{flux} values are listed in Table 5 and displayed on Fig. 10. Contrasting with the monotonous upward rise of TOC_{or} , C_{flux} first decreases

then shows an increase, even if the $1.16 \text{ g } C_{\text{org}}/\text{m}^2/\text{y}$ value obtained for the upper part of interval A is certainly an overestimation since, as it is indicated by the dashed line on Fig. 10, MAR probably decreased during deposition of the corresponding sediments.

To interpret the factors governing the evolution of C_{flux} , it is of vital importance to analyse the changes which occurred in the flux of terrestrial organic components and nutrient availability and to take into account the progressive deepening of the sea. Due to our poor knowledge of the first two of these factors, and the simplifications in assessment of MAR and TOC_{or} , only a qualitative interpretation can be attempted here.

The time period represented by intervals A and B₁ was characterized by a slowing down of deposition of terrigenous material (see Section 6.1.2). This decrease in terrigenous flux was certainly accompanied by a decrease in flux of land plant material, which contributed to the decrease of C_{flux} . On the other hand, it is likely that with increasing shore distance less and less nutrient transported by continental runoff reached the Cs 61 site that resulted in a progressive decrease of local C_{prod} . Finally, due to the deepening of the sea (Fig. 11), an increasingly smaller portion of planktic OM leaving the photic zone reached the bottom. Obviously all of these changes contributed to the decrease of C_{flux} .

The upward decrease of organic C/N ratio along the lower half of the section (Figs. 6 and 11) means that the relative weight of terrestrial organic components, depleted in nitrogen relative to marine organic components (Meyers, 1994) decreases upwards. This finding supports the above suggested decrease of flux of land plant material during deposition of intervals A and B₁.

A jump of C_{flux} happened at around B₁–B₂ boundary and its subsequent rise occurred in spite of the continuous, even if moderate deepening of the sea (Fig. 11). Consequently, it is explained by an increase of C_{prod} and/or increase of terrestrial OM flux.

An increase of C_{prod} is possible only if the amount of nutrients increases in the photic zone. It is worth to mention that a significant increase in C_{prod} that

occurred during deposition of the Tard Clay, a potential oil source rock in the Oligocene of the HPB, was suggested to be related to an intensification of liberation of nutrients from products of coeval pyroclastic activity (Brukner-Wein et al., 1990). Possibility of such a fertilization by release of nutrients from newly erupted volcanic ash particles in contact with ocean surface water has been experimentally documented by Frogner et al. (2001).

Zeolite and at least a part of plagioclase present in the Cs 61 section are of pyroclastic origin (Section 5.1). According to plagioclase contents (Table 2) and MAR values (Table 4), average mass accumulation rates of plagioclase (MAR_{plag}), prevailing during deposition of intervals A, B₁, B₂ and C were 0.62, 0.28, 1.33 and 1.75 g/m²/y. This about six fold increase in MAR_{plag} along B₁, B₂ and C intervals suggests an increasing contribution of pyroclastic material. The assumption of an increase in contribution of pyroclastic material agrees well with the fact that at the top of the section, at 402.5 m the first macroscopically recognizable tuff layer

is observed (Fig. 3). Consequently, alteration of newly erupted pyroclastic material fallen in the sea liberated more and more nutrients, resulting in a jump of C_{prod} , followed by its progressive increase.

However, it cannot be excluded that part of the C_{flux} jump and its subsequent rise were the result of an increase in the flux of terrestrial organic components, as part of an increase in delivery of terrigenous material, reflected by the increase of MAR.

It is worth to mention that C_{flux} estimated for interval C is close to C_{flux} values reported by Vető and Hetényi (1991) for two cored Tard Clay sections. The scenario described above is illustrated on the ideogram of Fig. 12.

The fact that the above proposed evolution of C_{flux} can be interpreted in agreement with the evolution of the studied part of the HPB is encouraging for further use of our approach for estimation of TOC_{or} .

Future studies on relationship between $\Delta\text{TOC}_{\text{sulf}}$ and $\Delta\text{TOC}_{\text{aer}}$ in recent marine sediments are needed for improving estimation of TOC_{or} .

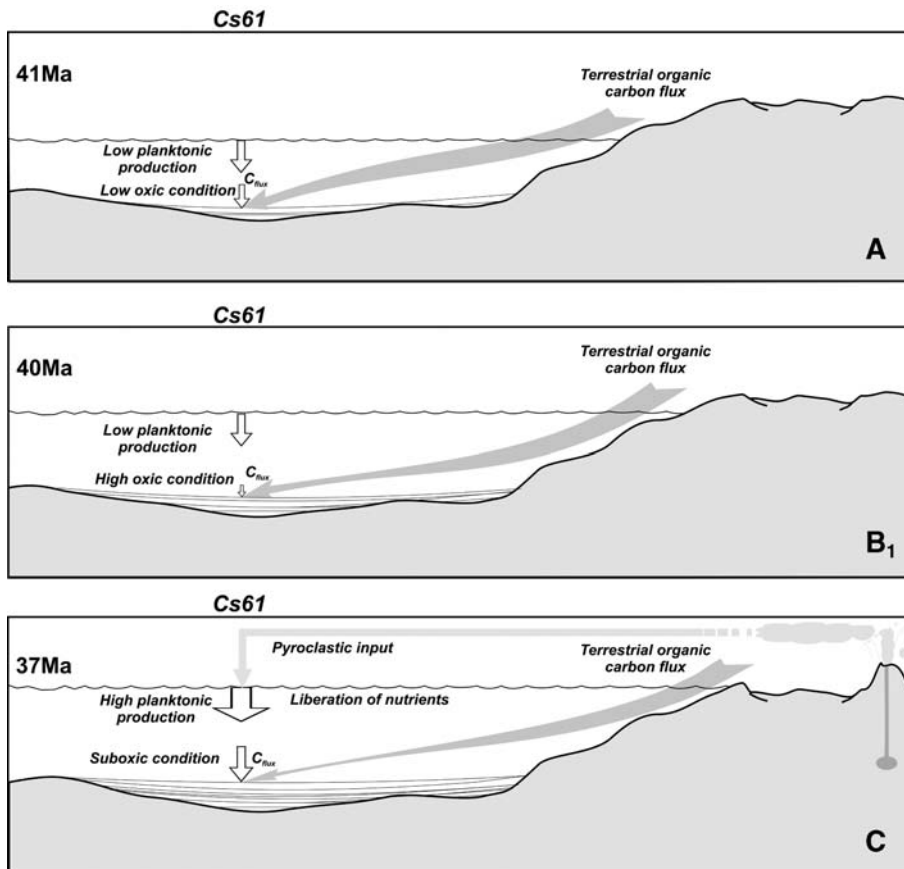


Fig. 12. Idealised scenario of evolution of C_{flux} and the main factors controlling it at the Cs 61 site during the Middle Eocene.

7. Conclusions

The new approach presented here, based on independent geochemical (TOC, sulphur content, $\delta^{34}\text{S}$), sedimentological (MAR) and palaeontological (BFOI and Q-mode (Varimax-rotated) factor analysis) data, permits to extend the calculation of C_{org} loss due to anaerobic respiration to oxic sediments. In case of high net sulphur isotope fractionation ($\Delta^{34}\text{S}_{\text{sulphate-sulphide}} > 45\%$) the obtained anaerobic C_{org} loss is underestimated. The new approach, with a higher degree of uncertainty, makes it possible to calculate C_{org} loss due to aerobic respiration. Again, in the case of high net sulphur isotope fractionation ($\Delta^{34}\text{S}_{\text{sulphate-sulphide}} > 45\%$) the obtained aerobic C_{org} loss is underestimated. Uncertainty of TOC_{or} estimation increases with increase of bottom water O_2 content and/or slowing down of sedimentation.

The evolution of C_{flux} during deposition of a Middle Eocene marly section, obtained using reconstructed original organic carbon content, can be qualitatively interpreted in terms of palaeobathymetry and availability of nutrients based on inferred changes in delivery of pyroclastic material into the sea.

Acknowledgements

This work was funded by a grant of the Hungarian Scientific Foundation (OTKA T 032260 and T042799). We thank József Pálffy for his comments on an earlier draft of this paper. The reviewing and helpful critical comments of two anonymous referees of *Paleo3* are greatly appreciated.

Appendix A. Supplementary data

Supplementary data associated with this article can be found, in the online version, at [doi:10.1016/j.palaeo.2006.12.001](https://doi.org/10.1016/j.palaeo.2006.12.001).

References

- Anderson, T.F., Pratt, L.M., 1995. Isotopic evidence for the origin of organic sulfur and elementary sulfur in marine sediments. In: Vairavamurthy, M.A., Schoenen, M.A.A. (Eds.), *Geochemical Transformation of Sedimentary Sulfur*. American Chemical Society Symposium Series, vol. 612, pp. 378–396.
- Báldi-Beke, M., 1984. The nannoplankton of the Transdanubian Palaeogene formations. *Geologica Hungarica. Series Palaeontologica* 43, 1–307.
- Báldi-Beke, M., Báldi, T., 1991. Palaeobathymetry and palaeogeography of the Bakony Eocene Basin in western Hungary. *Palaeogeography, Palaeoclimatology, Palaeoecology* 88, 25–52.
- Beier, J.A., Hayes, J.M., 1989. Geochemical and isotopic evidence for paleoredox conditions during deposition of the Devonian–Mississippian New Albany Shale, southern Indiana. *Geological Society of America Bulletin* 101, 774–782.
- Bernhardt, B., Báldi-Beke, M., Lantos, M., Horváth-Kollányi, K., Márton, P., 1988. Eocene magneto- and biostratigraphy at Somlóvásárhely, Hungary. *Acta Geologica Hungarica* 31, 33–52.
- Boltovskoy, E., Wright, R., 1976. *Recent Foraminifera*. W. Junk Publishers, The Hague. 515 pp.
- Bottrell, S.H., Parkes, R.J., Cragg, B.A., Raiswell, R., 2000. Isotopic evidence for anoxic pyrite oxidation and stimulation of bacterial sulphate reduction in marine sediments. *Journal of the Geological Society* 157, 711–714.
- Brüchert, V., Pérez, M.E., Lange, C.B., 2000. Coupled primary production, benthic foraminiferal assemblage, and sulfur diagenesis in organic-rich sediments of the Benguela upwelling system. *Marine Geology* 163, 27–40.
- Brukner-Wein, A., Hetényi, M., Vető, I., 1990. Organic geochemistry of an anoxic cycle: a case history from the Oligocene section, Hungary. *Organic Geochemistry* 15, 123–130.
- Burdett, J.W., Arthur, M.A., Richardson, M., 1989. A Neogene seawater sulfur isotope age curve from calcareous pelagic microfossils. *Earth and Planetary Science Letters* 94, 189–198.
- Buzas, M.A., Gibson, T.G., 1969. Species diversity: benthonic foraminifera in the western North Atlantic. *Science* 163, 72–75.
- Canfield, D.E., 1994. Factors influencing organic carbon preservation in marine sediments. *Chemical Geology* 114, 315–329.
- Canfield, D.E., Teske, A., 1996. Late Proterozoic rise in atmospheric oxygen concentration inferred from phylogenetic and sulphur-isotope studies. *Nature* 382, 127–132.
- Canfield, D.E., Thamdrup, B., 1994. The production of ^{34}S -depleted sulfide during bacterial disproportionation of elemental sulfur. *Science* 266, 1973–1975.
- Corliss, B.H., 1985. Microhabitats of benthic foraminifera within deep-sea sediments. *Nature* 314, 435–438.
- Corliss, B.H., 1991. Morphology and microhabitat preferences of benthic foraminifera from the northwest Atlantic Ocean. *Marine Micropaleontology* 17, 195–236.
- Corliss, B.H., Chen, C., 1988. Morphotype patterns of Norwegian Sea deep-sea benthic foraminifera and ecological implications. *Geology* 16, 716–719.
- Császár, G. (Ed.), 1997. *Basic Lithostratigraphic Units of Hungary. Charts and Short Descriptions*. The Geological Institute of Hungary, Budapest. 114 pp.
- Den Dulk, M., Reichart, G.J., Van Heyst, S., Zachariasse, W.J., Van der Zwaan, G.J., 2000. Benthic foraminifera as proxies of organic matter flux and bottom water oxygenation? A case history from the northern Arabian Sea. *Palaeogeography, Palaeoclimatology, Palaeoecology* 161, 337–359.
- Douglas, R.G., Woodruff, F., 1981. Deep-sea benthic foraminifera. The oceanic lithosphere. In: Emiliani, C. (Ed.), *The Sea*, pp. 1233–1237.
- Dunkl, I., 1990. Fission track dating of tuffaceous Eocene formations of the North Bakony Mountains (Transdanubia, Hungary). *Acta Geologica Hungarica* 33, 13–30.
- Durand, B., Monin, J.C., 1980. Elemental analysis of kerogens. In: Durand, B. (Ed.), *Kerogen*. Technip, Paris, pp. 113–142.
- Dymond, J., Suess, E., Lyle, M., 1992. Barium in deep-sea sediment: a geochemical proxy for paleoproductivity. *Paleoceanography* 7, 163–181.
- Frogner, P., Gislason, S.R., Óskarsson, N., 2001. Fertilizing potential of volcanic ash in ocean surface water. *Geology* 29, 487–490.
- Gibson, T.G., 1989. Planktic benthic foraminiferal ratios: modern patterns and Tertiary applicability. *Marine Micropaleontology* 15, 29–52.
- Goldhaber, M.B., Kaplan, I.R., 1980. Mechanism of sulfur incorporation and isotope fractionation during early diagenesis in sediments of the Gulf of California. *Marine Chemistry* 9, 95–143.

- Grimsdale, T.F., Van Morkhoven, F.P.C.M., 1955. The ratio between pelagic and benthic foraminifers as means of estimating depth of deposition of sedimentary rocks. *Proc. World. Pet. Congr.*, 4th Rome, pp. 473–491.
- Habicht, K.S., Canfield, D.E., 2001. Isotope fractionation by sulfate-reducing natural populations and the isotopic composition of sulfide in marine sediments. *Geology* 29, 555–558.
- Habicht, K.S., Canfield, D.E., Rethemier, J., 1998. Sulfur isotope fractionation during bacterial reduction and disproportionation of thiosulfate and sulfite. *Geochimica et Cosmochimica Acta* 62, 2585–2595.
- Halas, S., Shakur, A., Krouse, H.R., 1982. Modified method of SO₂ extraction from sulphates for isotopic analysis using NaPO₃. *Isotopenpraxis* 18, 433–435.
- Hardenbol, J., Thierry, J., Farley, M.B., Jacquin, Th., de Graciansky, P.C., Vail, P.R., 1998. Mesozoic and Cenozoic sequence chronostratigraphic framework of European basins. *SEPM Special Publication* 60 (364 pp.).
- Hertelendi, E., Gál, J., Paál, A., Fekete, S., Giurgiu, M., Gál, I., Kertész, Zs., Nagy, S., 1986. Stable isotope mass spectrometer. In: Stiehle, G. (Ed.), *Proc. 4th Working Meet., Isotopes in Nature*, Leipzig, vol. 1984, pp. 323–334.
- Horváth-Kollányi, K., 1983. Eocene planktic foraminifera zones from NE part of Transdanubian central range. *Földtani Közlemény (Bulletin of the Hungarian Geological Society)* 113, 225–236.
- Jorissen, F.J., De Stigter, H.C., Widmark, J.G.V., 1995. A conceptual model explaining benthic foraminiferal microhabitats. *Marine Micropaleontology* 26, 3–15.
- Jørgensen, B.B., 1990. A thiosulphate shunt in the sulfur cycle of marine sediments. *Science* 249, 152–154.
- Kaiho, K., 1991. Global changes of Paleogene aerobic/anaerobic benthic foraminifera and deep-sea circulation. *Palaeogeography, Palaeoclimatology, Palaeoecology* 83, 65–85.
- Kaiho, K., 1994. Benthic foraminiferal dissolved-oxygen index and dissolved-oxygen levels in the modern ocean. *Geology* 22, 719–722.
- Kaiho, K., 1999. Effect of organic carbon flux and dissolved oxygen on the benthic foraminiferal oxygen index (BFOI). *Marine Micropaleontology* 37, 67–76.
- Kaiho, K., Takeda, T., Petrizzo, M.R., Zachos, J.C., 2006. Anomalous shifts in tropical Pacific planktonic and benthic foraminiferal test size during the Paleocene–Eocene thermal maximum. *Palaeogeography, Palaeoclimatology, Palaeoecology* 237, 456–464.
- Kampschulte, A., Strauss, H., 2004. The sulfur isotopic evolution of Phanerozoic seawater based on the analysis of structurally substituted sulfate in carbonates. *Chemical Geology* 204, 255–286.
- Kaplan, I.R., Rittenberg, S.C., 1964. Microbiological fractionation of sulfur isotopes. *J. Genet. Microbiol.* 34, 195–212.
- Kaplan, I.R., Emery, K.O., Rittenberg, S.C., 1963. The distribution and isotopic abundance of sulfur in recent marine sediments off Southern California. *Geochimica et Cosmochimica Acta* 27, 297–331.
- Kázmér, M., Dunkl, I., Frisch, W., Kuhlmann, J., Ozsvárt, P., 2003. The Palaeogene forearc basin of the Eastern Alps and Western Carpathians: subduction erosion and basin evolution. *Journal of the Geological Society* 160, 413–428.
- KBFI, 1992. Petrophysical measurements on Eocene samples from Cs71 and Cs72 coreholes. *Hungarian Geological Survey Open File Report*, vol. 164/79.
- Kollányi, K., Bernhardt, B., Báldi-Beke, M., Lantos, M., 2003. An integrated stratigraphical examination of some Eocene boreholes of the Transdanubian Range (in Hungarian). *Földtani Közlemény (Bulletin of the Hungarian Geological Society)* 133, 69–90.
- Kristensen, E., Devol, H., Hartnett, H.E., 1999. Organic matter diagenesis in sediments on the continental shelf and slope of the Eastern Tropical and temperate North Pacific. *Continental Shelf Research* 19, 1331–1351.
- Lallier-Verges, E., Bertrand, P., Huc, Y., Bückel, D., Tremblay, P., 1993. Control of preservation of organic matter by productivity and sulphate reduction in Kimmeridgian shales from Dorset (UK). *Marine and Petroleum Geology* 10, 600–605.
- Leventhal, J.S., 1983. An interpretation of carbon and sulfur relationships in Black Sea sediments as indicators of environment of deposition. *Geochimica et Cosmochimica Acta* 47, 133–137.
- Littke, R., Baker, D.R., Leythaeuser, D., Rullkötter, J., 1991. Keys to the depositional history of the Posidonia Shale (Toarcian) in the Hils Syncline, Northern Germany. In: Tyson, R.V., Pearson, T.H. (Eds.), *Modern and Ancient Continental Shelf Anoxia Geological Society Special Publication*, vol. 50, pp. 311–333.
- Mackensen, A., Douglas, R.G., 1989. Down-core distribution of live and dead deep-water benthic foraminifera in box cores from Weddel Sea and the California Borderland. *Deep-Sea Research* 36, 879–900.
- Mackensen, A., Sejrup, H.P., Jansen, E., 1985. The distribution of living benthic foraminifera on the continental slope and rise off southwest Norway. *Marine Micropaleontology* 9, 275–306.
- Malmgren, B.A., Haq, B.U., 1982. Assessment of quantitative techniques in palaeobiogeography. *Marine Micropaleontology* 7, 213–236.
- Meyers, P.A., 1994. Preservation of elemental and isotopic source identification of sedimentary organic matter. *Chemical Geology* 114, 289–302.
- Mühlstrasser, T., 2001. Palaeoceanographic history of the Northwestern Tethyan Realm for the Late Oligocene through Middle Miocene. *Tübinger Mikropaläontologische Mitteilungen*, vol. 24, 119 pp.
- Murray, J.W., 1991. *Ecology and Palaeoecology of Benthic Foraminifera*. Longman, London, 397 pp.
- Nagymarosy, A., Báldi-Beke, M., 1988. The position of the Palaeogene formations of Hungary in the standard nannoplankton zonation. *Annales Universitatis Scientiarum Budapestinensis. Sectio Geologica* 28, 3–25.
- Naidu, P.D., Malmgren, B.A., 1995. Do benthic foraminifer records represent a productivity index in oxygen minimum zone areas? An evaluation from the Oman Margin, Arabian Sea. *Marine Micropaleontology* 26, 49–55.
- Oberhänsli, H., Müller-Merz, E., Oberhänsli, R., 1991. Eocene paleoceanographic evolution at 20–30° S in the Atlantic Ocean. *Palaeogeography, Palaeoclimatology, Palaeoecology* 83, 173–215.
- Orr, W.L., 1986. Kerogen/asphaltene/sulfur relationships in sulfur-rich Monterey oils. *Organic Geochemistry* 10, 499–516.
- Ozsvárt, P., 2003. Palaeoceanographic history of the Hungarian Palaeogene Basin during the Eocene. PhD dissertation, Eötvös University, Budapest 182 pp.
- Passier, H.F., Bosch, H.-J., Nijenhuis, I.A., Lourens, L.J., Böttcher, M.E., Leenders, A., Sinninghe Damsté, J.S., de Lane, G., de Leeuw, J.W., 1999. Sulphidic Mediterranean surface waters during Pliocene sapropel formation. *Nature* 397, 146–149.
- Paytan, A., Kastner, M., Campbell, D., Thiemens, M.H., 1998. Sulfur isotopic composition of Cenozoic seawater sulfate. *Science* 282, 1459–1462.
- Raiswell, R., 1997. A geochemical framework for the application of stable sulphur isotopes to fossil pyritization. *Journal of the Geological Society* 154, 343–356.

- Rozanov, A.G., Volkov, I.I., Zhabina, N.N., Jagodinskaja, T.A., 1971. Serovodorod v osadkah beregovo sklona severo-zapadnoj chasti Tihogo Okeana. *Geohimija* 543–550.
- Scherbacher, M., Schmiedl, G., Hemleben, Ch., 2001. Early Oligocene benthic foraminifera from the Lower Inn Valley area: implications for the paleoenvironmental evolution of the Inneralpine Molasse. In: Piller, W.E., Rasser, M.W. (Eds.), *Paleogene of the Eastern Alps*. Österr. Akad. Wiss., Schriftenr. Erdwiss. Komm, Wien, pp. 611–640.
- Schippers, A., Jørgensen, B.B., 2002. Biogeochemistry of pyrite and iron sulfide oxidation in marine sediments. *Geochimica et Cosmochimica Acta* 66, 85–92.
- Schmiedl, G., Mackensen, A., Müller, P.J., 1997. Recent benthic foraminifera from the eastern South Atlantic Ocean: dependence on food supply and water masses. *Marine Micropaleontology* 32, 249–287.
- Schmiedl, G., Scherbacher, M., Bruch, A.A., Jelen, B., Nebelsick, J., Hemleben, Ch., Mosbrugger, V., Rifel, H., 2002. Paleoenvironmental evolution of the Paratethys in the Slovenian Basin during the Late Paleogene. *International Journal of Earth Sciences* 91, 123–132.
- Schott, W., 1935. Die Foraminiferen in dem Äquatorialen Teil des Atlantischem Ozeans. *Deutsche Atlantische Expedition* 6, 411–416.
- Torres, M.E., Brumsack, H.J., Bohrmann, G., Emeis, K.C., 1996. Barite fronts in continental margin sediments: a new look at barium remobilization in the zone of sulfate reduction and formation of heavy barites in diagenetic fronts. *Chemical Geology* 127, 125–139.
- Van der Zwaan, G.J., Duijnste, I.A.P., Den Dulk, M.S., Ernst, R., Jannik, N.T., Kouwenhoven, T.J., 1999. Benthic foraminifers: proxies or problems? A review of palaeoecological concepts. *Earth-Science Reviews* 46, 213–236.
- Vető, I., Hetényi, M., 1991. Fate of organic carbon and reduced sulphur in dysoxic anoxic Oligocene facies of the Central Paratethys (Carpathian Mountains and Hungary). In: Tyson, R.V., Pearson, T. H. (Eds.), *Modern and Ancient Continental Shelf Anoxia*. Geological Society Special Publication, vol. 50, pp. 449–460.
- Vető, I., Hetényi, M., Demény, A., Hertelendi, E., 1995. Hydrogen index as reflecting sulphidic diagenesis in non-bioturbated shales. *Organic Geochemistry* 22, 299–310.
- Vető, I., Hetényi, M., Hámor-Vidó, M., Hufnagel, H., Haas, J., 2000. Anaerobic degradation of organic matter controlled by productivity variation in a restricted Late Triassic basin. *Organic Geochemistry* 31, 439–452.
- Vinogradov, A.P., Grinenko, V.A., Ustinov, V.I., 1962. Isotopic composition of sulphur compounds in the Black Sea. *Geokhimija* 10, 973–997.
- Wollenburg, J.E., Mackensen, A., 1998. Living benthic foraminifers from the central Arctic Ocean: faunal composition, standing stock and diversity. *Marine Micropaleontology* 34, 153–185.
- Zaback, D.A., Pratt, L.M., Hayes, J.M., 1993. Transport and reduction of sulphate and immobilization of sulfide in marine black shale. *Geology* 21, 141–144.